Molecular imaging of protein kinase activity and its application in diseases

by

Limin Zhang

A dissertation submitted in partial fulfillment
of the requirements for degree of
Doctor of Philosophy
(Toxicology)
in The University of Michigan
2009

Doctoral Committee:

Professor Alnawaz Rehemtulla, Co-Chair
Professor Craig Harris, Co-Chair
Professor Martin Philbert
Professor Brian D. Ross
Associate Professor Mats Ljungman

Acknowledgements

My time at the University of Michigan has tremendous impacts on me, and for this I would like to thank many individuals. My advisor, Professor Alnawaz Rehemtulla, led me into this exciting area, encouraged me to explore new topics and gave me guidance. I benefited a lot from his insight, expertise and valuable scientific discussion with him, while I was still given sufficient freedom to conduct my projects. I am grateful to him for training me in every aspect to become a scholar. My committee member, Professor Brian Ross, provided me great opportunity to learn the cutting-edge technologies of molecular imaging and helped me with my *in vivo* imaging experiments. The other members of my committee, Professors Craig Harris, Martin Philbert and Mats Ljungman, have provided valuable advice and support during the dissertation process.

I have made many good friends in Ann Arbor, I would especially thank my labmates, who gave me help and encouraged me through this pursuit. Christin Hamilton, helped me with many experiments, and most importantly, she helped me go through some difficult times; Mahaveer Swaroop Bhojani taught me many molecular biology techniques, presentation and writing skills, as well as gave me appropriate advice on my projects; Shama Virani, Kuei Lee, and Craig Galban helped me with *in vivo* imaging experiments.

I would also like to thank my husband, Xiulin Ruan and my parents, without their support and understanding this work would not have been possible. The especial thank would be made to my son, Gavin Ruan, who lightened my life and made this pursuit more joyful.

This work is supported by US National Institutes of Health grants P01CA85878, P50CA01014 and R24CA83099 and a Leob Predoctoral Fellowship from NIH and a Predoctoral Fellowship from Rackham Graduate School at the University of Michigan.

Table of Contents

List of Figures

Abstract

Protein kinases are important regulators of signaling pathways. Dysregulation of protein kinases can be triggered by a variety of stimuli (such as environmental toxins) and is associated with a number of human disorders, making them attractive targets for the development of molecular therapies. Developing tools which allow real time, non-invasive, dynamic and quantitative imaging of kinase activity will facilitate a better understanding of biological processes in the cellular and molecular levels and provide a solid foundation for rational kinase inhibitor design. In this work, a new reporter platform based on complementation of firefly luciferase was described for monitoring kinase (Akt and Met) activity in living subjects.

The Ser/Thr kinase Akt mediates mitogenic and anti-apoptotic sequelae that result from activation of multiple signaling cascades. The Akt pathway is considered as a key determinant of biologic aggressiveness of tumors, and a major target for novel anti-cancer therapies. Using bioluminescent Akt reporter, Akt activity in cultured cells and in tumor xenografts was monitored quantitatively and dynamically in response to receptor tyrosine kinase activation or inhibition, as well as direct inhibition of Akt. A bioluminescent reporter based on the same platform was also generated to study receptor tyrosine kinase Met. Met and its ligand hepatocyte growth factor/scatter factor (HGF/SF) modulate signaling cascades implicated in cellular migration, invasion, proliferation, survival, and angiogenesis that are root of cancer cell dysregulation including cellular

proliferation, therapeutic resistance and metastasis in various human malignancies. Using bioluminescent Met reporter, Met activity in response to the inhibition of the HGF/Met signaling pathway via a Met kinase inhibitor and an HGF neutralizing antibody was studied in a glioma model. To monitor protein kinase activity in the tissue dependent manner, a Cre-mediated transgenic mouse model expressing bioluminescent Akt reporter was ultimately generated wherein Akt kinase activity can be monitored non-invasively in the cells and tissues that have undergone Cre-mediated recombination.

Results obtained from these studies provided unique insights into the pharmacokinetics and pharmacodynamics of agents that modulate kinase activity, allowed development of optimal dosing and schedule parameters for maximal tumor control in cancer treatment, and validated protein kinase as a target for brain cancer therapy. The transgenic mouse model will enable the study of protein kinases in response to cellular stress in the tissue of interest. If combined with existing Cre-mediated cancer mouse model, such transgenic mouse model will allow the non-invasive and longitudinal study of tumor growth and therapeutic response using bioluminescence imaging. This work demonstrates that bioluminescence reporter assays provided novel methodologies to study protein kinases. Such assays will greatly aid in the characterization of molecular events in mammalian cells, enable the screening of compounds which inhibit kinase activation and pave the way for discovery of novel clinical therapies.

Chapter 1

Introduction

Protein kinases in health and disease

Protein kinases are enzymes that covalently attach a phosphate group donated by ATP to a specific amino acid residue on protein substrates. The human genome contains about 500 protein kinase genes which consist of about 2% of all eukaryotic genes[1]. These protein kinases regulate up to 30% of all proteins. Based on the amino acids they phosphorylate, protein kinases are classified into different families. Two main eukaryotic kinases are serine/threonine-specific kinases and tyrosine-specific kinases, which phosphorylate hydroxyamino acids of serine/threonine or tyrosine respectively. These kinases have been indicated in the regulation of most of aspects of cellular function in mammalian cells. Another type of protein kinases is histidine protein kinase which phosphorylates downstream substrates on the imidazole nitrogens of histidine. Histidine protein kinases regulate responses to stimuli in prokaryotic and lower eukaryotic cells[2,3]. In this work, serine/threonine specific kinases and tyrosine specific kinases will be discussed.

Phosphorylation of target residues in proteins by protein kinases results in changes in protein activity, cellular location and interaction with other proteins. These changes launches a chain of intracellular protein interactions that modulate gene transcription and

cell response. Protein phosphorylation catalyzed by kinases play an important role in mediating intracellular signal-transduction pathways in a range of processes from embryogenesis to cell death[4].

Dysregulation of protein kinases has been implicated in more than 400 human diseases such as cancer, rheumatoid arthritis, cardiovascular and neurological disorders, asthma and psoriasis[4-9]. Therefore, these enzymes make a very attractive target for therapeutic interventions. It is no surprise that the first molecularly targeted drug, Gleevec (imatinib), used in treatment of chronic myelogenous leukemia (CML) and gastrointestinal stromal tumors (GISTs) is a tyrosine kinase inhibitor[10]. For the treatment of human malignancies, a number of kinase inhibitors are being developed and are under various stages of preclinical or clinical investigation[11].

Serine/threonine-specific kinases

Serine/threonine-specific kinases are a group of enzymes that phosphorylate serine or threoine residues in the target proteins. These protein kinases are involved in many signaling cascades related to cell cycle regulation and growth control.

MAPKs

MAPKs are ubiquitously expressed enzymes connecting cell-surface receptors to essential cellular targets. MAPKs regulate growth factor signaling cascades thereby controlling cell survival and adaptation. The MAPKs family consists of MAPKs, MAPK kinases (MAPKKs, MKKs or MEKs) and MAPK kinase kinases or MEK kinases (MKKKs or MEK kinases), which constitute the three-kinase phospho-relay system. MKKKs (or MEK kinases) phosphorylate and activate MAPKKs (or MKKs, MEKs), which in turn phosphorylate and activate MAPKs[12]. This three-kinase phospho-relay

system is modulated by STE20 kinases or small GTO-binding proteins[13]. In mammalian cells, there are at least five known MAPKs family: (ERK)-1/2, Jun amino-terminal kinases (JNK1/2/3), p38 proteins (p38a/b/g/d), ERK5, and ERK7[14]. Each MAPK is activated by specific MAPKK. For example, ERK1/2 is phosphorylated and activated by MEK1/2; p38 is activated by MKK3/6. Each MAPKK, however, can be activated by more than one MAPKKK, which further contribute to the complexity of the system.

The MAPKs family regulates various cellular processes in response to a plethora of extracellular stimuli, including cytokines, antigens, toxins, stress insults and cell-cell interactions[15]. They are activated by dual phosphorylation of both threonine and tyrosine residues. Once activated, each MAPK phosphorylates a number of substrates which are composed of serine or threonine followed by a proline, and the surrounded amino acids to increase the specificity of the recognition by the catalytic pocket of the enzyme[16].

One of the most studied functions of MAPKs is the regulation of gene expression. JNKs phosphorylate and activate Jun proteins to form AP-1 complexes with fos[17]; p38 phosphorylates and activates MEF2C protein and related family members[18]. MAPKs are also involved in cell proliferation, cell survival and death, and cell motility. Since MAPKs play such essential role in transduction of intracellular signals, deregulated MAPKs have been indicated in many diseases, such as inflammation, rheumatoid arthritis, diabetes, Parkinson's and Alzheimer's diseases[19].

CDKs

Cyclin-dependent kinases (CDKs) are a large family of heterodimeric serine/threonine protein kinases which are originally found to be involved in the regulation of cell cycle. The hallmark of CDKs is that the catalytic activity of CDKs

requires the association with regulatory subunits called cyclins[20]. There are 14 putative CDKs and 34 putative cyclins encoded in the human genome[21].

CDKs is modulated by a serial of mechanisms, including synthesis of cyclins, formation of cyclin/ CDK complexes, phosphorylation and inactivation by kinases (Wee1 and Myt1), dephosphorylation and activation by phosphatases (cdc25), binding of CDK inhibitor (CIP/KIP family), and ubiquitin-mediated degradation of cyclins and CDK inhibitors (SCF ubiquitin ligase and the APC/C)[22]. Once activated, CDKs drive the cell cycle from one phase to the next. Different CDKs form active complexes with different cyclins at different phases of the cell cycle. Briefly, cyclin D interacts with CDK4 and CDK6 and functions primarily during G1 phase of the cell cycle; cyclin E forms complexes with CDK2 to regulate G1/S-transition; The complexes of cyclin A with CDK1 and CDK2 during S and G2 phases play positive roles in replication and passage through G2; Cdk1 associates with cyclin B during G2 phase to modulate many of the events required for mitosis[23-25].

CDKs also regulate transcription, DNA repair, and postmitotic processes. For example, CDK2, CDK3, CDK4 and CDK6 are involved in the phosphorylation of retinoblastoma susceptibility protein (Rb), activation of E2F transcription factors, and DNA replication[25].

Dysregulation of CDKs is involved in many pathological processes. Most human malignances carry gene alterations in upstream regulators or downstream targeting substrates of CDKs. For example, CDK2 and CDK4 are amplified in lung cancers. Over-expression of CDKs 2, 3, 4 and 6 results in the loss of Rb function, in turn leads to carcinogenesis[26].

PKB/Akt

In the past, scientists have focused on the central importance of RAS in the field of cancer research. In recent years, phosphoinositide-3 kinase (PI-3K) and Akt pathway has been recognized as another important regulator of mammalian cell proliferation and survival.

The serine/threonine kinase PKB/Akt is composed of an amino-terminal PH domain, a central catalytic domain and a short carboxy-terminal regulatory domain. The activation of Akt is regulated by both translation to the plasma membrane and phosphorylation at Thr 308 and Ser473. PKB/Akt functions as a signaling hub wherein many upstream signaling pathways such as IGF-1R, HER2/Neu, PDGF-R, HGF-R converge (**Fig. 1.1**). Through the phosphorylation of many downstream effectors, such as NF-kappa B, mTOR, Forkhead, Bad, GSK-3 and MDM-2 [4,27-34], Akt mediates cell growth, proliferation, and survival[18,30,35,36]. Because Akt is deregulated in a wide range of human cancers, the Akt pathway is considered as a major target for anti-cancer therapies[37-40]. Ongoing efforts have focused on therapeutically targeting Akt itself or its upstream regulators and downstream effectors[41-53].

Tyrosine-specific kinases

Tyrosine kinase family is the largest subgroup of human protein kinases. There are over 90 known protein tyrosine kinase genes in human genome. Of the 90 tyrosine kinase genes, 58 encode transmemberane receptor tyrosine kinases (RTKs) divided into 20 subfamilies; 32 encode cytoplasmic non-receptor tyrosine kinases (NRTKs) grouped into 10 subfamilies[4]. Tyrosine kinases are involved in many aspects of mammalian

development; therefore they play etiologic roles in the initiation of many human diseases. They have become the most studied group of protein kinases.

Non receptor tyrosine kinasese (NRTKs)

Most NRTKs localize in the cytoplasm and serve as integral components of RTKs and other receptors by transducing extracellular signals to downstream intermediates in pathways. Some NRTKs are anchored to the cell memberane by myristoylation or palmitoylation[45]. Most NRTKs contain a tyrosine kinase domain, Src homology 2 (SH2) and 3 (SH3) domains. The SH2 domain is a phosphorylation binding domain which binds to phosphorylated tyrosine residues. The SH3 domain binds to the proline-rich peptide of their specific partners. NRTK is activated by the tyrosine phosphorylation via trans-autophosphorylation or cis - phosphorylation by a different NRTK. Activation of the NRTK initiates the phosphorylation of cytoplasmic substrates thus resulting in the activation of targeted proteins and the production of second messenger molecules, which are transmitted into the nucleus and regulate gene transcription.

NRTKs play a crucial rule in many aspects of multicellular communication and development, including the response to extracellular stimuli, T- cell and B-cell activation, and cytoskeleton restructuring, mitogenesis, cell survival and apoptosis, transcriptional regulation[54,55]. Therefore dysregulation of NRTKs is involved in many diseases, such as cancer. Indeed, v-Src, which belongs to the biggest subfamily in NRTKs, was the first proto-oncogene discovered.

Receptor tyrosine kinases (RTKs)

Receptor tyrosine kinases (RTKs) are transmembrane glycoproteins composed of an extracellular ligand-binding domain and an intracellular tyrosine kinase domain linked

by a drophobic transmembrane domain. RTKs are activated by binding of ligands thus induce receptor dimerization and autophosphorylation of the intracellular tyrosine kinase domain. Activation of RTKs initiates a series of signaling events including the recruitment of SH2 domain-containing proteins to the specific tyrosine residues and phosphorylation of targeted proteins.

RTKs modulate a plethora of signaling cascades in mammalian cells, including cell growth and survival, neovascularization, tissue repair and regeneration. Consequently, dysregulation of the RTKs compromises the cellular capacity to moderate these activities, and leads to the initiation and progress of many tumor types. Deregulation of RTKs (eg. EGFR and Met) results in constitutive activation of downstream effectors including Ras and PI-3K/Akt pathways. A number of kinase inhibitors for receptor tyrosine kinases have been developed by the pharmaceutical industry and academic institutions[56].

EGFR

Epidermal growth factor receptor (EGFR) is a member of a type I TK family which includes four receptor tyrosine kinases, ErbB-1 (EGFR), ErbB-2 (Her-2), ErbB-3, and ErbB-4. The EGFR transmembrane glycoprotein consists of an extracellular ligand-binding domain, a transmembrane domain and intracellular tyrosine kinase domain. EGFR has several ligands, the best-known ligands of EGFR are EGF and transforming growth factor-a (TGF-a)[57]. Ligand binds to EGFR, induces receptor dimerization and autophosphorylation which leads to the initiation of signaling cascades involved in cell proliferation and survival. Activated EGFR recruits and phosphorylates a number of signaling molecules, including phospholipase C-c (PLC-c), Ras, phosphatidylinositol-3 kinase (PI-3K), and STAT3[54].

Overexpression of EGFR has been observed in a wide range of solid tumors, including 40-80% non small cell lung cancers (NSCLCs), glioblastoma, head and neck cancers, prostate cancers[58]. The magnitude of EGFR signaling is affected by several cellular mechanisms, including overexpression of the ligand or EGFR, gene mutations, or transactivation through receptor dimerization[54]. Small molecular inhibitors of EGFR such as Erlobinib have been used clinically to inhibit the EGFR signalling pathway and additionally potentiate the effectiveness of traditional anti-cancer therapy.

Met (HGF receptor)

Met is a prototypic member of receptor tyrosine kinases and was discovered as an activated oncogene. It is the only known high-affinity receptor for HGF (or SF)[59]. HGF was characterized as a potent motility factor and a platelet-derived mitogen for hepatocytes[60]. HGF and c-Met are widely expressed in a variety of tissues. Met receptor is expressed in epithelial cells, while HGF is secreted by mesenchymal cells and accumulates ubiquitously in tissues[61]. HGF binds to Met, induces receptor homodimrization, and leads to the autophosphorylation of multiple tyrosine residues in the kinase domain and at its docking sites. Phosphorylation of Met recruits a number of adapter signaling molecules, including Grb2, Shc, Gab1, Crk/CRKL, phosphatidylinositol 3-kinase (PI3K), and Src. Recruitment of Shc and Grb2 implicates the involvement of Ras-mitogen-activated protein kinase pathways; recruitment of PI-3K indicates the activation of phosphatidylinositol 3-kinase-Akt signaling pathway[62] (**Fig. 1.2**). Through the regulation of downstream effectors, Met/HGF pathway mediates a plethora of normal cellular activities, including cellular migration, invasion, proliferation, survival, and angiogenesis[63].

Dysregulation of Met/HGF pathway leads to cellular proliferation, therapeutic resistance and metastasis in various human malignancies. A variety of mechanisms inducing aberrant Met activation have been characterized, including genetic mutation, receptor amplification or ligand-dependent autocrine or paracrine, or structural rearrangements[64]. Inappropriate activation of Met/HGF has been seen in many human malignancies, including brain cancer, colon cancer, renal carcinoma, and lung cancer[65]. Clinical studies showed bad prognostic outcomes from patients carrying upregulated HGF and/or Met. The therapeutic abrogation of HGF/Met receptor coupling or Met receptor-mediated signaling events may provide promising clinical insights into more effective strategies for preventing tumor growth and spread.

As one of the major post-translational modification mechanisms, protein phosphorylation controls a variety of cellular regulatory processes. Protein phosphorylation is crucial in regulating normal cellular activities that are at the root of cell dysregulation, which leads to many human diseases including cancers, diabetes, neurological and cardiovascular disorders. As a reversible process, phosphorylation is governed by combined actions of protein kinases and protein phosphatases.

Protein phosphatases

Protein phosphatases are enzymes, which remove phosphate groups from substrate residues. Based upon their substrate specificity, phosphatases can be classified into two major groups, tyrosine-specific phosphatases and serine/threonine-specific phosphatases. In addition, some phosphatases possess dual specificity for both tyrosine and serine/threonine. Other types of phosphatases include histidine phosphatase, which dephosphorylates phospho-histidine in prokaryotic and lower eukaryotic cellular

responses, and lipid phosphatase which dephosphorylates phosphatidyl-inositol-3,4,5-triphosphate. Protein tyrosine phosphatases (PTPs) contain a signature motif (H/V)C(X)$_5$R(S/T) along with a range of structural domains, including SH2, PDZ, and ligand binding domains. PTPs are further categeried into two classes, receptor-like and intracellular PTPs. The receptor-like PTPs are characterized with extracellular ligand-binding domain, transmembrane region, and cytoplasmic PTP domain. The intracellular PTPs generally have catalytic domain and various amino or carboxyl terminal extentions containing SH2 domains[66,67]. Protein serine/threonine phosphatases are subdivided into PPP family, which dephosphorylates phosphoserine and includes the most abundant protein serine/threonine phosphatases PP2A and PP2B, and PPM family, which contains PP2C and the related mitochondrial pyruvate dehydrogenase phosphatases. Within each family, the individual protein phosphatase is created as a combination of various regulatory domains and subunits[68].

Protein phosphatases were initially defined as housing keeping enzymes which dephosphoylate any enzymes they encountered. Recently research has found that they are tightly mediated. Even the remarkable progress in the understanding of protein phosphatases, the molecular basis of which substrate protein phosphatases recognize is still undefined. Based on the studies of protein phosphatase substrates using synthetic peptides, it has been found that most protein phosphatases exhibit a spectrum of substrate specificity, except for the dual-specificity phosphatases which have more stringent substrate specificity.

Protein phosphatases play essential roles in a variety of signaling pathways and the abberent activation of protein phosphatases can contribute to the pathogenesis of

many human diseases. Consequently, inhibitors targeted to protein phosphatases have been developed and yielded successes. However, two major issues related to specificity made it difficult to use phosphatase inhibitors for treating diseases. Until recently inhibitors targeting oncogenic protein phosphatases such as Cdc25 have been used successfully for cancer therapy in the clinic.

As discussed above, protein kinases regulate most of cellular events. Dysregulation of protein kinases is involved in a plethora disorders and have been connected to over 400 diseases. The elucidation of protein kinase activity will contribute not only to a better understanding of the signal transduction cascades, but also to the development of novel therapeutic agents. Existing modalities for monitoring Akt activity utilize techniques such as western blotting or immunocytochemistry using a phospho-specific target antibody, and in vitro kinase assays. However, these methods are invasive, cumbersome, and only provide a "snap-shot" view of the kinase activity at a specific time point. So the technologies to dynamically and quantitatively monitor and quantify kinase activity are urgently needed.

Molecular imaging of Protein kinases

Molecular imaging is defined as a non–invasive visual representation of biological processes at the cellular and molecular level in the whole organism while also encompassing the modalities and instrumentation to support the visualization and measurement of these processes[69]. This is an attempt to bridge the gap between discovery of important disease biomarkers and their use in clinical. In the last decade, at least three different molecular imaging technologies have been utilized for the understanding of disease biomarkers, drug development or monitoring therapeutic outcome, which are (1)

optical imaging (bioluminescence and fluorescence imaging) (2) Magentic resonance imaging (MRI) and (3) Nuclear imaging [e.g. single photon emission computed tomography (SPECT) and positron emission tomography (PET)]. They have emerged as powerful tools that enable real time and repetitive visualization of gene expression, signal transduction, protein-protein interaction, and cell trafficking in intact cells and living animals. This emerging field of molecular imaging promises to bring in novel tools for the dynamic measurement of signaling cascades and its players thereby eliminating the needs for time-consuming dissection and histological methods for tissue analysis and longitudinal studies of biological processes. Molecular imaging tools provide non-invasive real time, dynamic imaging and quantification of kinase activity in living cells and subjects. These tools can aid in preclinical determination of drug dosage, schedule and combination. Further, since an increase in kinase activity is synonymous with cancer cell proliferation and tumor growth while the reduction of kinase activity is associated with decreased tumorgenicity, molecular imaging of kinase activity could be exploited as a surrogate marker for monitoring real time response of cancer cells to therapeutic regimens. The applications of molecular imaging assays *in vitro* also provide an excellent platform for cell based high throughput screening. Inhibitors identified by such assays typically pass the barriers of solubility, membrane permeability and toxicity, thus enhancing their chance of being successful in experimental and clinical investigation. In summary, the development of molecular imaging tools for kinases would significantly enhance our understanding of the biology of cancer and assist in the development and evaluation of novel therapeutic agents.

Protein Complementation Assays

We have recently described the development of a bioluminescent Akt reporter which can be used to measure Akt phosphorylation in cultured cells and mice[69]. This reporter was based on conformation dependent complementation of firefly luciferase. Protein complementation assays have their roots in protein engineering strategies wherein a monomeric reporter is split into two separate inactive components in such a way that when these components are brought into close proximity they reconstitute the original reporter activity. Protein complementation has been extensively exploited to understand protein-protein interaction. Historically, the yeast two hybrid system first described by Stan Fields[70] is based on protein complementation of GAL4, a transcriptional activator protein. This discovery revolutionized the understanding of signaling cascades in eukaryotic organisms. Although, a plethora of interacting partners in a variety of signaling cascades was discovered, this system has limited utility in dissecting mammalian signaling pathways. A number of other reporters routinely utilized in understanding mammalian biology were engineered for complementation studies. These include fluorescent proteins (GFP and YFP) [71], bioluminescent enzymes (Firefly luciferase and renilla luciferase), β-galactosidase, dihydrofolate reductase (DHFR) and TME1 β-lactamase.

Of the different complementation assays, the bioluminescence reporter has emerged as a useful technique for small animal imaging. Luciferase is a photoprotein which modifies the substrate (luciferin) releasing photons in the presence of oxygen and ATP. The light emitted by Firefly luciferase appears blue to yellow green in color with an emission spectra that peaks at wavelength between 490 nm to 620 nm[72]. There are more than 30 luciferase-luciferin systems of independent origin but the most utilized luciferase

for in vivo molecular imaging is the ATP-dependent firefly (Photinus pyalis) luciferase[73]. This is chiefly due to the fact that 30% of the light generated by firefly luciferase has an emission spectra above 600 nm, a region where the signal attenuation by the absorption and scattering properties of mammalian tissue is minimal[73,74]. This is a major advantage compared to other optical imaging systems such as fluorescence imaging wherein the excitation light can also excite other naturally occurring fluorescent molecules in the body which may result in a high level of background autofluorescence.

An optimized firefly luciferase protein fragment complementation was developed by screening incremental truncation libraries of N- and C-terminal fragments of luciferase[75]. The N-terminal and C-terminal luciferase fragments were fused with FRB of the mammalian target of rapamycin and FK506-binding protein 12 (FKBP), respectively. The optimized pair of FRB-NLuc/CLuc-FKBP reconstituted luciferase activity upon single-site binding of rapamycin in an FK506-competitive manner. By employing this strategy, the investigators monitored the lower affinity protein-protein interaction, such as the phosphorylation-dependent interaction between human Cdc25C with 14-3-3ε in vivo. Paulmerugan et al., designed a complementation-based assay using renilla luciferase by exploiting the strong interaction of MyoD and Id[76]. Recently, a non-ATP dependent Gaussia princeps luciferase enzyme was engineered for protein complementation assay and demonstrates cross talk between insulin and TGFβ signaling pathways [77].

Kinase Imaging by Fluorescence Resonance Energy Transfer

A number of groups have reported development of tools to monitor kinase activity such as serine/threonine kinase PKA, PKB, PKC, PKD and non-receptor tyrosine kinase Src in live mammalian cells by fluorescence resonance energy transfer (FRET) [35,78-81].

FRET is a mechanism by which energy is transferred from an excited donor fluorohore to an acceptor fluorophore when the two are in close proximity. The typical strategy for kinase imaging is based on conformational change induced by phosphorylation such that the phosphorylation brings the acceptor and donor fluorphores in close proximity resulting in FRET. Using this strategy, Sasaki[82] described kinase reporter wherein the phosphorylation dependent intermolecular binding results in changes in fluorescence. The reporters contain two green fluorescent protein mutants, an Akt substrate, and a phosphorylation recognition domain. Phosphorylation of the Akt substrate in the reporter causes a change in FRET, allowing the detection of phosphorylation catalyzed by Akt. They used the endogenous Akt substrate nitric-oxide synthase and Bad, which were fused with the Golgi targeting domain and mitochondria targeting domain. By using these reporters, they suggested that activated Akt is localized to subcellular compartments, including the Golgi apparatus and/or mitochondria, rather than diffusing into the cytosol, thereby resulting in efficient phosphorylation of its substrate proteins. A similar strategy was also used by Kunkel et al to monitor Akt activity in the cytosol and nucleus[78]. They found that Akt signaling in the cytosol is more rapid and transient when compared to Akt signaling in the nucleus which indicates the possibility of differentially regulated phosphatase activity between these two compartments. Additionally, targeting the reporter to the plasma membrane, where Akt is activated, resulted in an accelerated and a prolonged response compared to the cytosol, suggesting that release of Akt or its substrates from the membrane is required for desensitization of Akt signaling. In summary, the novel biology of kinases has been deciphered through the use of FRET based kinase reporters in vitro.

Kinase Imaging Using a Bioluminescent Reporter

With the goal of monitoring kinase activity *in vivo*, we have developed a split firefly luciferase based reporter wherein Akt activity can be measured by bioluminescence imaging[69]. A hybrid polypeptide, BAR, was constructed in which an Akt consensus substrate peptide and phosphoamino acid binding domain (FHA2) are flanked by the amino- (N-Luc) and carboxyl- (C-Luc) terminal domains of the firefly luciferase reporter molecule. In the presence of Akt kinase activity, phosphorylation of the Akt consensus substrate sequences within the reporter results in its interaction with the FHA2 domain, thus stearically preventing reconstitution of a functional luciferase reporter molecule. In the absence of Akt kinase activity, release of this stearic constraint allows reconstitution of the luciferase reporter molecule whose activity can be detected non-invasively by BLI. In contrast to the FRET-based reporters, which allow reporter activity to be monitored in single cells, the split luciferase reporter allows imaging in live cells and animals in a quantitative, dynamic and non-invasive manner. The inhibition of Akt activity using an Akt inhibitor (API-2) and a PI-3K inhibitor (perifosine) resulted in an increase of bioluminescence activity in a time- and dose-dependent manner, which indicates that BAR provides a surrogate for Akt activity in terms of quantity and dynamics. BAR was also used to study upstream signaling events of Akt. For example, stimulation of EGFR can be evaluated using Akt activity as a surrogate and monitored by bioluminescent imaging. The use of an EGFR inhibitor, erlotinib with an erlotinib-sensitive and an erlotinib-resistant cell lines resulted in differential activation of the BAR reporter.

The ability to non-invasively and quantitatively image Akt activity within a specific tissue in live animals significantly enhanced our understanding of pharmacokinetics and bioavailability of specific drugs. For example, at 40 mg/kg API-2 treatment, inhibitory levels of the compound were detected for up to 24 hours which decreased thereafter. In contrast, when 20 mg/kg was delivered, peak inhibition was detected at 12 hours and by 24 hours little inhibitory activity was detected. In contrast to API-2 for which published pharmacokinetics data are not available, the pharmacokinetics of perifosine has been extensively studied. Published data demonstrated that high plasma concentrations of the drug could be detected for as long as seven days post treatment. Results obtained from the BAR reporter studies in live animals confirm this observation since high levels of Akt inhibitory activity was detected within two hours of treatment which remained elevated for seven days.

Molecular imaging of protein kinases in cells and live animals will greatly facilitate the process of target validation, dose and schedule optimization as well as for rapid identification of a lead compounds from a library using cell based high throughput screening. This technology will facilitate the determination of pharmacokinetics and pharmacodynamics of drugs in mice which may or may not be of relevance in humans. It provides a unique opportunity to design the optimal dosing and schedule regiments for maximal tumor control and minimal normal tissue toxicity.

Integration of genetically encoded imaging reporters into cells and animals has provided a unique opportunity to monitor molecular, biochemical, and cellular pathways in vivo. It will greatly facilitate the process of target validation and dose and schedule

optimization, as well as providing a way to identify lead compounds from a library using cell-based, high-throughput screening.

Figure legends

Figure 1.1 PI-3K/Akt signaling pathway. Phosphoinositide 3-kinase (PI-3K) is activated through stimulation of receptor tyrosine kinases (RTKs). Once activated, PI-3K catalyses the conversion of Ptdlns(4,5)P_2 (PIP2) to Ptdlns(3,4,5)P_2 (PIP3) which recruites Akt to cell membrane and helps to activate Akt. The activated Akt by PDK1 mediates several cellular targets, such as MDM2, mTOR, GSK3β, NF-κB, FKHR and BAD. The regulation of these targets results in increased cellular growth, survival, proliferation, and decreased apoptosis.

Figure 1.2 Met signaling pathway. Met receptor is activated by the binding of HGF ligand and the autophosphorylation of multiple tyrosine residues in the kinase domain and at its docking sites. The activation of Met recruits a number of adapter signaling molecules, including Grb2, Shc, Gab1, phosphatidylinositol 3-kinase (PI3K), Src and STAT3. Recruitment of Shc and Grb2 activates Ras-mitogen-activated protein kinase pathways; recruitment of PI-3K triggers the activation of phosphatidylinositol 3-kinase-Akt signaling pathway.

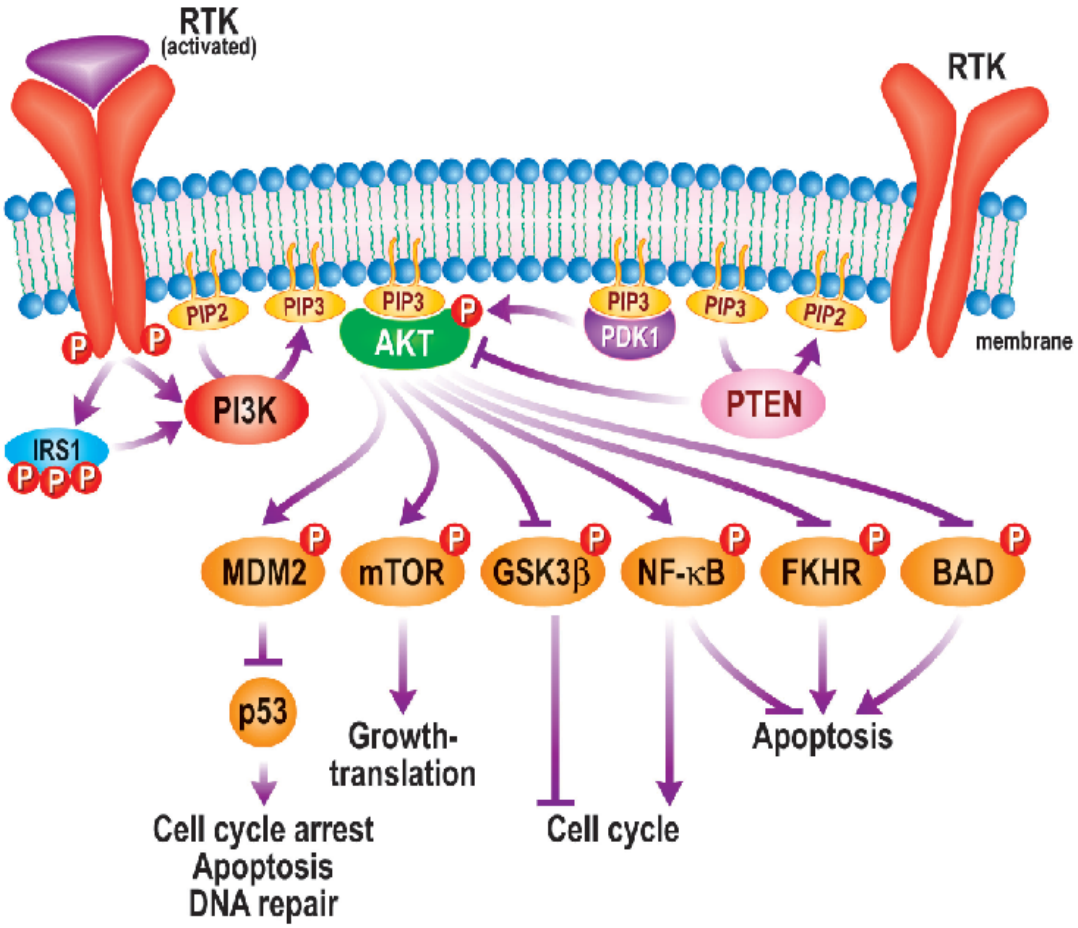
RTK
(activated)
RTK
membrane
PIP2
PIP3
PIP3
AKT
PIP3
PDK1
PIP3
PIP2
PI3K
PTEN
IRS1
MDM2
mTOR
GSK3β
NF-κB
FKHR
BAD
p53
Growth-
translation
Apoptosis
Cell cycle arrest
Apoptosis
DNA repair
Cell cycle

Figure 1.1

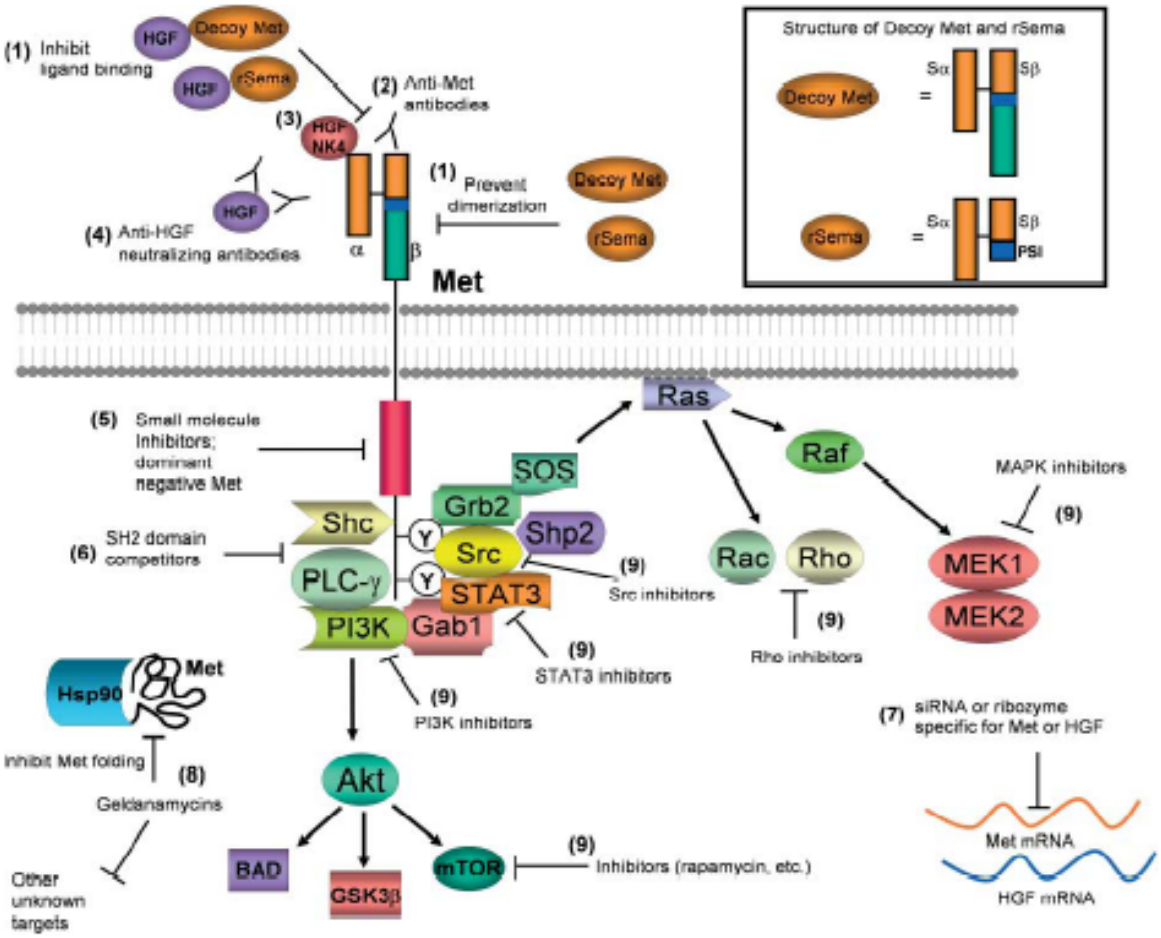
(1) Inhibit ligand binding
HGF
Decoy Met
HGF
rSema
(2) Anti-Met antibodies
(3)
HGF NK4
(4) Anti-HGF neutralizing antibodies
HGF
α
β
(1) Prevent dimerization
Decoy Met
rSema
Met
Structure of Decoy Met and rSema
Decoy Met
Sα
Sβ
rSema
Sα
Sβ
PSI
(5) Small molecule inhibitors; dominant negative Met
(6) SH2 domain competitors
Shc
PLC-γ
PI3K
Grb2
SOS
Src
Shp2
STAT3
Gab1
Ras
Raf
MEK1
MEK2
MAPK inhibitors
(9)
Rac
Rho
(9)
Rho inhibitors
(9)
Src inhibitors
(9)
STAT3 inhibitors
(9)
PI3K inhibitors
Hsp90
Met
Inhibit Met folding
(8)
Geldanamycins
Other unknown targets
Akt
BAD
GSK3β
mTOR
(9)
Inhibitors (rapamycin, etc.)
(7) siRNA or ribozyme specific for Met or HGF
Met mRNA
HGF mRNA

Figure 1.2

References

1. Manning, B.D. & Cantley, L.C. AKT/PKB signaling: navigating downstream. *Cell* **129**, 1261-74 (2007).

2. Steeg, P.S., Palmieri, D., Ouatas, T. & Salerno, M. Histidine kinases and histidine phosphorylated proteins in mammalian cell biology, signal transduction and cancer. *Cancer Lett* **190**, 1-12 (2003).

3. Besant, P.G. & Attwood, P.V. Mammalian histidine kinases. *Biochim Biophys Acta* **1754**, 281-90 (2005).

4. Blume-Jensen, P. & Hunter, T. Oncogenic kinase signalling. *Nature* **411**, 355-65 (2001).

5. Westra, J. & Limburg, P.C. p38 mitogen-activated protein kinase (MAPK) in rheumatoid arthritis. *Mini Rev Med Chem* **6**, 867-74 (2006).

6. Kumar, R., Singh, V.P. & Baker, K.M. Kinase inhibitors for cardiovascular disease. *J Mol Cell Cardiol* **42**, 1-11 (2007).

7. Mueller, B.K., Mack, H. & Teusch, N. Rho kinase, a promising drug target for neurological disorders. *Nat Rev Drug Discov* **4**, 387-98 (2005).

8. Blease, K. Targeting kinases in asthma. *Expert Opin Investig Drugs* **14**, 1213-20 (2005).

9. Ben-Bassat, H. Biological activity of tyrosine kinase inhibitors: novel agents for psoriasis therapy. *Curr Opin Investig Drugs* **2**, 1539-45 (2001).

10. Radford, I.R. Imatinib. Novartis. *Curr Opin Investig Drugs* **3**, 492-9 (2002).

11. Dancey, J. & Sausville, E.A. Issues and progress with protein kinase inhibitors for cancer treatment. *Nat Rev Drug Discov* **2**, 296-313 (2003).

12. English, J. et al. New insights into the control of MAP kinase pathways. *Exp Cell Res* **253**, 255-70 (1999).

13. Gutkind, J.S. Regulation of mitogen-activated protein kinase signaling networks by G protein-coupled receptors. *Sci STKE* **2000**, RE1 (2000).

14. Johnson, G.L., Dohlman, H.G. & Graves, L.M. MAPK kinase kinases (MKKKs) as a target class for small-molecule inhibition to modulate signaling networks and gene expression. *Curr Opin Chem Biol* **9**, 325-31 (2005).

15. Shchemelinin, I., Sefc, L. & Necas, E. Protein kinases, their function and implication in cancer and other diseases. *Folia Biol (Praha)* **52**, 81-100 (2006).

16. Chang, L. & Karin, M. Mammalian MAP kinase signalling cascades. *Nature* **410**, 37-40 (2001).

17. Treisman, R. Regulation of transcription by MAP kinase cascades. *Curr Opin Cell Biol* **8**, 205-15 (1996).

18. Han, J., Jiang, Y., Li, Z., Kravchenko, V.V. & Ulevitch, R.J. Activation of the transcription factor MEF2C by the MAP kinase p38 in inflammation. *Nature* **386**, 296-9 (1997).

19. Waetzig, V. & Herdegen, T. Context-specific inhibition of JNKs: overcoming the dilemma of protection and damage. *Trends Pharmacol Sci* **26**, 455-61 (2005).

20. Schang, L.M. Advances on cyclin-dependent kinases (CDKs) as novel targets for antiviral drugs. *Curr Drug Targets Infect Disord* **5**, 29-37 (2005).

21. Liu, J. & Kipreos, E.T. Evolution of cyclin-dependent kinases (CDKs) and CDK-activating kinases (CAKs): differential conservation of CAKs in yeast and metazoa. *Mol Biol Evol* **17**, 1061-74 (2000).

22. Harper, J.W. & Adams, P.D. Cyclin-dependent kinases. *Chem Rev* **101**, 2511-26 (2001).

23. Reed, S.I. Control of the G1/S transition. *Cancer Surv* **29**, 7-23 (1997).

24. Sherr, C.J. Cancer cell cycles. *Science* **274**, 1672-7 (1996).

25. Malumbres, M. & Barbacid, M. Mammalian cyclin-dependent kinases. *Trends Biochem Sci* **30**, 630-41 (2005).

26. Blagden, S. & de Bono, J. Drugging cell cycle kinases in cancer therapy. *Curr Drug Targets* **6**, 325-35 (2005).

27. Romashkova, J.A. & Makarov, S.S. NF-kappaB is a target of AKT in anti-apoptotic PDGF signalling. *Nature* **401**, 86-90 (1999).

28. Brunn, G.J. et al. Direct inhibition of the signaling functions of the mammalian target of rapamycin by the phosphoinositide 3-kinase inhibitors, wortmannin and LY294002. *Embo J* **15**, 5256-67 (1996).

29. Sarbassov, D.D., Guertin, D.A., Ali, S.M. & Sabatini, D.M. Phosphorylation and regulation of Akt/PKB by the rictor-mTOR complex. *Science* **307**, 1098-101 (2005).

30. Brunet, A. et al. Akt promotes cell survival by phosphorylating and inhibiting a Forkhead transcription factor. *Cell* **96**, 857-68 (1999).

31. Zha, J., Harada, H., Yang, E., Jockel, J. & Korsmeyer, S.J. Serine phosphorylation of death agonist BAD in response to survival factor results in binding to 14-3-3 not BCL-X(L). *Cell* **87**, 619-28 (1996).

32. Cross, D.A., Alessi, D.R., Cohen, P., Andjelkovich, M. & Hemmings, B.A. Inhibition of glycogen synthase kinase-3 by insulin mediated by protein kinase B. *Nature* **378**, 785-9 (1995).

33. Mayo, L.D. & Donner, D.B. A phosphatidylinositol 3-kinase/Akt pathway promotes translocation of Mdm2 from the cytoplasm to the nucleus. *Proc Natl Acad Sci U S A* **98**, 11598-603 (2001).

34. Vivanco, I. & Sawyers, C.L. The phosphatidylinositol 3-Kinase AKT pathway in human cancer. *Nat Rev Cancer* **2**, 489-501 (2002).

35. Wang, Y. et al. Visualizing the mechanical activation of Src. *Nature* **434**, 1040-5 (2005).

36. Carroll, P.E. et al. Centrosome hyperamplification in human cancer: chromosome instability induced by p53 mutation and/or Mdm2 overexpression. *Oncogene* **18**, 1935-44 (1999).

37. Cheng, J.Q. et al. Amplification of AKT2 in human pancreatic cells and inhibition of AKT2 expression and tumorigenicity by antisense RNA. *Proc Natl Acad Sci U S A* **93**, 3636-41 (1996).

38. Ruggeri, B.A., Huang, L., Wood, M., Cheng, J.Q. & Testa, J.R. Amplification and overexpression of the AKT2 oncogene in a subset of human pancreatic ductal adenocarcinomas. *Mol Carcinog* **21**, 81-6 (1998).

39. Bellacosa, A. et al. Molecular alterations of the AKT2 oncogene in ovarian and breast carcinomas. *Int J Cancer* **64**, 280-5 (1995).

40. Staal, S.P. Molecular cloning of the akt oncogene and its human homologues AKT1 and AKT2: amplification of AKT1 in a primary human gastric adenocarcinoma. *Proc Natl Acad Sci U S A* **84**, 5034-7 (1987).

41. Hennessy, B.T., Smith, D.L., Ram, P.T., Lu, Y. & Mills, G.B. Exploiting the PI3K/AKT pathway for cancer drug discovery. *Nat Rev Drug Discov* **4**, 988-1004 (2005).

42. Rosenzweig, K.E., Youmell, M.B., Palayoor, S.T. & Price, B.D. Radiosensitization of human tumor cells by the phosphatidylinositol3-kinase

inhibitors wortmannin and LY294002 correlates with inhibition of DNA-dependent protein kinase and prolonged G2-M delay. *Clin Cancer Res* **3**, 1149-56 (1997).

43. Ng, S.S., Tsao, M.S., Nicklee, T. & Hedley, D.W. Wortmannin inhibits pkb/akt phosphorylation and promotes gemcitabine antitumor activity in orthotopic human pancreatic cancer xenografts in immunodeficient mice. *Clin Cancer Res* **7**, 3269-75 (2001).

44. Kim, S.H. et al. Potentiation of chemosensitivity in multidrug-resistant human leukemia CEM cells by inhibition of DNA-dependent protein kinase using wortmannin. *Leuk Res* **24**, 917-25 (2000).

45. Hubbard, S.R. & Till, J.H. Protein tyrosine kinase structure and function. *Annu Rev Biochem* **69**, 373-98 (2000).

46. Knight, Z.A. et al. Isoform-specific phosphoinositide 3-kinase inhibitors from an arylmorpholine scaffold. *Bioorg Med Chem* **12**, 4749-59 (2004).

47. Ward, S.G. & Finan, P. Isoform-specific phosphoinositide 3-kinase inhibitors as therapeutic agents. *Curr Opin Pharmacol* **3**, 426-34 (2003).

48. DeFeo-Jones, D. et al. Tumor cell sensitization to apoptotic stimuli by selective inhibition of specific Akt/PKB family members. *Mol Cancer Ther* **4**, 271-9 (2005).

49. Lindsley, C.W. et al. Allosteric Akt (PKB) inhibitors: discovery and SAR of isozyme selective inhibitors. *Bioorg Med Chem Lett* **15**, 761-4 (2005).

50. Barnett, S.F. et al. Identification and characterization of pleckstrin-homology-domain-dependent and isoenzyme-specific Akt inhibitors. *Biochem J* **385**, 399-408 (2005).

51. Kondapaka, S.B., Singh, S.S., Dasmahapatra, G.P., Sausville, E.A. & Roy, K.K. Perifosine, a novel alkylphospholipid, inhibits protein kinase B activation. *Mol Cancer Ther* **2**, 1093-103 (2003).

52. Van Ummersen, L. et al. A phase I trial of perifosine (NSC 639966) on a loading dose/maintenance dose schedule in patients with advanced cancer. *Clin Cancer Res* **10**, 7450-6 (2004).

53. Ouyang, W. et al. PI-3K/Akt pathway-dependent cyclin D1 expression is responsible for arsenite-induced human keratinocyte transformation. *Environ Health Perspect* **116**, 1-6 (2008).

54. Kolibaba, K.S. & Druker, B.J. Protein tyrosine kinases and cancer. *Biochim Biophys Acta* **1333**, F217-48 (1997).

55. Vlahovic, G. & Crawford, J. Activation of tyrosine kinases in cancer. *Oncologist* **8**, 531-8 (2003).

56. Perona, R. Cell signalling: growth factors and tyrosine kinase receptors. *Clin Transl Oncol* **8**, 77-82 (2006).

57. Raizer, J.J. HER1/EGFR tyrosine kinase inhibitors for the treatment of glioblastoma multiforme. *J Neurooncol* **74**, 77-86 (2005).

58. Raymond, E., Faivre, S. & Armand, J.P. Epidermal growth factor receptor tyrosine kinase as a target for anticancer therapy. *Drugs* **60 Suppl 1**, 15-23; discussion 41-2 (2000).

59. Bottaro, D.P. et al. Identification of the hepatocyte growth factor receptor as the c-met proto-oncogene product. *Science* **251**, 802-4 (1991).

60. Birchmeier, C., Birchmeier, W., Gherardi, E. & Vande Woude, G.F. Met, metastasis, motility and more. *Nat Rev Mol Cell Biol* **4**, 915-25 (2003).

61. Tsarfaty, I. et al. The Met proto-oncogene mesenchymal to epithelial cell conversion. *Science* **263**, 98-101 (1994).

62. Furge, K.A., Zhang, Y.W. & Vande Woude, G.F. Met receptor tyrosine kinase: enhanced signaling through adapter proteins. *Oncogene* **19**, 5582-9 (2000).

63. Zhang, Y.W. & Vande Woude, G.F. HGF/SF-met signaling in the control of branching morphogenesis and invasion. *J Cell Biochem* **88**, 408-17 (2003).

64. Boccaccio, C. & Comoglio, P.M. Invasive growth: a MET-driven genetic programme for cancer and stem cells. *Nat Rev Cancer* **6**, 637-45 (2006).

65. Toschi, L. & Janne, P.A. Single-agent and combination therapeutic strategies to inhibit hepatocyte growth factor/MET signaling in cancer. *Clin Cancer Res* **14**, 5941-6 (2008).

66. Zhang, Z.Y. Protein tyrosine phosphatases: structure and function, substrate specificity, and inhibitor development. *Annu Rev Pharmacol Toxicol* **42**, 209-34 (2002).

67. den Hertog, J., Ostman, A. & Bohmer, F.D. Protein tyrosine phosphatases: regulatory mechanisms. *Febs J* **275**, 831-47 (2008).

68. Barford, D. Molecular mechanisms of the protein serine/threonine phosphatases. *Trends Biochem Sci* **21**, 407-12 (1996).

69. Zhang, L. et al. Molecular imaging of Akt kinase activity. *Nat Med* **13**, 1114-9 (2007).

70. Fields, S. & Song, O. A novel genetic system to detect protein-protein interactions. *Nature* **340**, 245-6 (1989).

71. Ghosh, I., Hamilton, A.D. & Regan, L. Antiparallel leucine zipper-directed protein reassembly: Application to the green fluorescent protein. *Journal of the American Chemical Society* **122**, 5658-5659 (2000).

72. McCaffrey, A., Kay, M.A. & Contag, C.H. Advancing molecular therapies through in vivo bioluminescent imaging. *Mol Imaging* **2**, 75-86 (2003).

73. Greer, L.F., 3rd & Szalay, A.A. Imaging of light emission from the expression of luciferases in living cells and organisms: a review. *Luminescence* **17**, 43-74 (2002).

74. Contag, C.H. & Bachmann, M.H. Advances in in vivo bioluminescence imaging of gene expression. *Annu Rev Biomed Eng* **4**, 235-60 (2002).

75. Luker, K.E. et al. Kinetics of regulated protein-protein interactions revealed with firefly luciferase complementation imaging in cells and living animals. *Proc Natl Acad Sci U S A* **101**, 12288-93 (2004).

76. Paulmurugan, R. & Gambhir, S.S. Monitoring protein-protein interactions using split synthetic renilla luciferase protein-fragment-assisted complementation. *Anal Chem* **75**, 1584-9 (2003).

77. Remy, I. & Michnick, S.W. A highly sensitive protein-protein interaction assay based on Gaussia luciferase. *Nat Methods* **3**, 977-9 (2006).

78. Kunkel, M.T., Ni, Q., Tsien, R.Y., Zhang, J. & Newton, A.C. Spatio-temporal dynamics of protein kinase B/Akt signaling revealed by a genetically encoded fluorescent reporter. *J Biol Chem* **280**, 5581-7 (2005).

79. Kunkel, M.T., Toker, A., Tsien, R.Y. & Newton, A.C. Calcium-dependent regulation of protein kinase D revealed by a genetically encoded kinase activity reporter. *J Biol Chem* **282**, 6733-42 (2007).

80. Violin, J.D., Zhang, J., Tsien, R.Y. & Newton, A.C. A genetically encoded fluorescent reporter reveals oscillatory phosphorylation by protein kinase C. *J Cell Biol* **161**, 899-909 (2003).

81. Zhang, J., Ma, Y., Taylor, S.S. & Tsien, R.Y. Genetically encoded reporters of protein kinase A activity reveal impact of substrate tethering. *Proc Natl Acad Sci U S A* **98**, 14997-5002 (2001).

82. Sasaki, K., Sato, M. & Umezawa, Y. Fluorescent indicators for Akt/protein kinase B and dynamics of Akt activity visualized in living cells. *J Biol Chem* **278**, 30945-51 (2003).

Chapter 2
Molecular imaging of Akt kinase activity

Abstract

The Ser/Thr kinase Akt mediates mitogenic and anti-apoptotic sequelae that result from activation of multiple signaling cascades. The Akt pathway is considered a key determinant of biologic aggressiveness of tumors, and a major target for novel anti-cancer therapies. Here we describe the development of a reporter molecule wherein bioluminescence activity within live cells and animals can be used as a surrogate for Akt activity. Akt activity within tumor cells in culture as well as in tumor xenografts was monitored quantitatively and dynamically in response to API-2 and Perifosine, two small molecules that inhibit Akt activity by two distinct mechanisms. In addition, the activation of Akt in response to growth factor receptor activation as well as inhibition of Akt in response to treatment of cells with receptor tyrosine kinase inhibitors was also imaged quantitatively and dynamically over time. The results provided unique insights into the pharmacokinetics and pharmacodynamics of agents that modulate Akt activity which can be used to develop optimal dosing and schedule parameters for optimal efficacy.

Introduction

The serine/threonine kinase PKB/Akt functions as a signaling hub wherein many upstream signaling pathways converge[1]. The integration of these intracellular signals at the level of Akt and its kinase activity, regulate the phosphorylation of several downstream effectors, such as NF-kappa B, mTOR, Forkhead, Bad, GSK-3 and MDM-2 [2-9]. These phosphorylation events in turn mediate the effects of Akt on cell growth, proliferation, protection from pro-apoptotic stimuli, and stimulation of neo-angiogenesis[5,10]. Because Akt and its upstream regulators are dysregulated in cancer, they serve as promising targets for pharmaceutical intervention[11-17].

Molecular imaging techniques bridge the gap between preclinical and clinical research for the development of candidate drugs that have target specificity, optimal pharmacodynamics and efficacy[18-20]. The use of molecular imaging endpoints instead of time-consuming dissection and histology significantly decreases the workload as imaging is non-invasive, allows for longitudinal studies in a single animal with improved statistical relevance. In the present study we describe the development of a reporter molecule which provides the ability to non-invasively image Akt activity using bioluminescence imaging (BLI). Using this reporter, the efficacy and bioavailability of modulators of signaling pathways that impinge on Akt were investigated *in vitro* as well as in live animals.

Results

Construction of BAR, a bioluminescent Akt reporter

To enable non-invasive detection of Akt activity in live cells and animals, we constructed a hybrid polypeptide, BAR (**Fig. 2.1a**). This molecule constitutes, an Akt consensus substrate peptide, a phosphoamino acid binding domain (FHA2)[21] flanked by the amino-(N-Luc) and carboxyl-(C-Luc) terminal domains of the firefly luciferase reporter molecule[22]. In addition to the wild type reporter (BAR*wt*), two additional reporters were also constructed (**Fig. 2.1a**), one that had a key threonine residue (Thr596) mutated to alanine (BAR*mut1*) and a second that had all potential threonine and serine residues (Ser590, Ser594 and Thr596) within the substrate peptide mutated to alanine (BAR*mut2*). The functional basis of the reporter is schematically shown in **Fig. 2.1b**. In the presence of Akt kinase activity, phosphorylation of the Akt consensus substrate sequence within the reporter would result in its interaction with the FHA2 domain, thus stearically preventing reconstitution of a functional luciferase reporter molecule. In the absence of Akt kinase activity, releasing of this stearic constrain would allow reconstitution of the luciferase reporter molecule whose activity can be detected non-invasively by bioluminescence imaging (BLI).

To demonstrate that the expected polypeptides were expressed from the recombinant DNA constructs, each of the expression plasmids was transfected into mammalian cells and western blot analysis was performed (**Fig. 2.1c**). D54 human glioma cells expressing the full length luciferase molecule yielded a 61 kD polypeptide, while cells expressing the BAR*wt*, BAR*mut1*, as well as BAR*mut2* yielded an 84 kD anti-luciferase reactive polypeptide. These polypeptides resulting from the luciferase

expression vector as well as each of the BAR (based on a 2292 bp open reading frame constituting 764 amino acids) expression vectors were of the expected molecular weight. Mock transfected D54 cells failed to show a luciferase specific polypeptide.

Stable cell lines were constructed using the expression vectors for each of the above reporters, to investigate if inhibition of Akt activity would result in changes in bioluminescence activity. As shown in **Fig. 2.1d**, treatment of D54-Luciferase cells with an Akt inhibitor (API-2) did not result in a significant change in bioluminescence activity, while treatment of D54-BAR*wt* cells resulted in a three fold increase in bioluminescence activity, D54-BAR*mut1* cells as well as D54-BAR*mut2* had no significant change in bioluminescence activity in response to API-2 treatment.

Western blot analysis revealed that API-2 treatment resulted in inhibition of Akt as visualized by the loss of reactivity with a phospho-Akt specific antibody but not with an antibody specific for total Akt (**Fig. 2.1e**). These results demonstrate that Akt is constitutively active in D54 cells and inhibitable by API-2. As shown in **Fig. 2.1f**, treatment of DU145-BAR*wt* cells but not DU145-luciferase cells or BAR*mut1* and BAR*mut2* cells with API-2 resulted in a 3.5 fold induction of bioluminescence activity. Western blot analysis of Akt in these cells confirmed that API-2 treatment resulted in inhibition of Akt activity (**Fig. 2.1g**). We also investigated the ability of the BAR reporter to detect changes in Akt status upon stimulation of growth factor receptors. To investigate the ability of the reporter to detect changes in Akt status in response to activation of EGFR, UMSCC-1 cells expressing the BAR*wt* reporter were serum starved overnight and treated with EGF or with 20% serum. Within 10 mins of treatment, a 3-4 fold decrease in bioluminescence activity was detected (**Fig. 2.1h**). Western blot analysis

of these cells revealed that at this time point there was a corresponding increase in phospho-Akt levels but not total Akt (**Fig. 2.1i**). Interestingly, treatment of cells with EGF resulted in increased phospho-EGFR levels compared to total EGFR (**Fig. 2.1i**), which was not observed when cells were treated with serum. GAPDH specific antibody was used to demonstrate equal loading.

Dose and time dependent imaging of Akt activity

To evaluate the activity of the BAR reporter as a quantitative and dynamic surrogate for Akt activity, D54-BAR*wt* cells were treated with various doses of API-2 and imaged at various times. **Fig. 2.2a** demonstrates that bioluminescence activity increased in a dose dependent manner for the first five minutes and plateaud thereafter. At the highest dose of API-2, a peak was observed at 5 mins followed by a small decline. Western blot analysis of these samples validated the bioluminescence reporter in that a dose dependent decrease of phospho-Akt (but not total Akt) levels was observed (**Fig. 2.2b**) and in addition, a time dependent decrease in phospho-Akt was also observed (**Fig. 2.2c**).

D54-BAR*wt* cells were also treated with various doses of Perifosine, a lipophilic small molecule that inhibits Akt activity[16]. As shown in **Fig. 2.2d**, treatment of D54-BAR*wt* cells with Perifosine resulted in a dose and time dependent increase in bioluminescence activity. These changes in bioluminescence activity correlated with phospho-Akt levels as determined by western blot analysis (**Fig. 2.2e**). The western blots (**Fig. 2.2b, 2.2c and 2.2e**) demonstrate that treatment with the above two drugs did not result in changes in total Akt levels while a dose and time dependent change in phospho-

Akt levels was observed. In **Fig. 2.2e**, we also demonstrate that changes in bioluminescence activity were not due to changes in the levels of the reporter.

Phosphorylation of BAR is dependent on Akt activity

To further investigate if BAR was phosphorylated in an Akt dependent manner, we treated D54-BAR*wt* cells with API-2, 30 mins after treatment, the cells were imaged for bioluminescence activity (**Fig. 2.3c**). Cell extracts were prepared from parallel plates and used to immunoprecipitate the reporter molecular using an anti-luciferase antiserum. The immunoprecipitate was resolved using SDS-PAGE and western blotted using a phospho-threonine specific antibody. As shown in **Fig. 2.3a**, the BAR protein had significantly lower levels of phospho-threonine in the presence of Akt inhibitors which correlated with a decrease in phospho-Akt levels (and therefore Akt activity, **Fig. 2.3b**). A decrease in the phophorylation of the Akt protein and the resulting decrease in phosphorylation of the BAR protein correlated with an increase in bioluminescence activity.

To evaluate the specificity of the BAR reporter, D54-BARwt expressing cells were treated with rapamycin and LY294002, two well known serine/threonine kinase inhibitors with specificity for mTOR and PI-3K respectively. Rapamycin treatment did not result in a significant change in BLI activity while treatment with LY294002 resulted in a 6 fold induction of BLI activity (**Fig. 2.3d**). These results were consistent with the observation that rapamycin treatment did not affect phospho-Akt levels, while LY294002 almost completely inhibited phosphorylation of Akt (**Fig. 2.3e**). Analysis of the p70S6K protein in these cells revealed that both rapamycin and LY294002 inhibited phosphorylation of this mTOR target as expected.

Biological imaging of Akt

To test the utility of the BAR reporter in a biological context, we utilized lung cancer cell lines HCC827 and NCI-H1975 which have differential sensitivity to erlotinib due to mutations within the EGFR sequence[23]. Treatment of the erlotinib sensitive cell line HCC827 with erlotinib resulted in a 6 fold induction of BLI activity compared to pretreatment, while the erlotinib resistant NCI-H1975 cells revealed no significant increase in BLI activity (**Fig. 2.4a**). Western blot analysis validated that treatment of HCC827 cells but not NCI-H1975 cells with erlotinib resulted in a decrease in EGFR activity as detected by phospho-EGFR levels compared to total EGFR level (**Fig. 2.4b**). Correspondingly HCC827 cells but not NCI-H1975 cells responded to erlotinib treatment as detected by phospho-Akt levels compared to total-Akt levels. To further validate this observation, cell viability experiment revealed that HCC827 cells had a significant decrease in cell proliferation while NCI-H1975 cells did not have a significant change in cell proliferation at the treated doses of erlotinib (**Fig. 2.4c and 2.4d**).

The ability of an agent to modulate its target's activity in vivo is dependent on multiple factors. The pharmacokinetics and bioavailability of the drug within the whole body and within the tumor has a significant impact on the optimal dosing and schedule of drug required for maximal target modulation. To investigate if the BAR reporter can be used to interrogate Akt status within a tumor in response to a specific agent, we implanted D54-BARwt cells into the flanks of SCID mice to establish tumors. When tumors were 40-60 mm3 in volume, bioluminescence activity was monitored in animals treated with an Akt inhibitor or vehicle controls over time. As shown in **Fig. 2.4e**, bioluminescence activity remained essentially flat over a 48 hour period in vector treated

animals. In contrast, in API-2 treated animals bioluminescence activity increased within the first two hours and reached a peak within 6 hours. Animals treated with low doses of drug (20 mg/kg) had a very small increase in bioluminescence activity and this change in activity subsided within 120 mins. In contrast, in animals treated with 40 mg/kg, a much greater change in bioluminescence activity was detected, which was found to stay elevated for a longer period of time (**Fig.2.4e**). These results suggest that doses in excess of 40 mg/kg of API-2 were required for optimal pharmacokinetics and pharmacodynamics.

In contrast to API-2, which according to the results described above has a plasma half life of minutes, Perifosine, based on published results, has a very long plasma half life in mice[24]. To investigate if the BAR reporter validated this observation, mice implanted with D54-BAR*wt* tumors were treated with 30 mg/kg Perifosine. As shown in **Fig. 2.4f**, in response to Perifosine, bioluminescence activity increased within 6 hours of treatment and remained high for over 7 days (data not shown). A representative image of a mouse in each treatment group is shown in **Fig. 2.4g**.

To confirm that the differences in bioluminescence activity in these animals was due to changes in Akt phosphorylation status, representative tumors were resected from a vector treated animal as well as API-2 and Perifosine treated animals at 6 hour time point. Immunohistochemical staining using a phospho-Akt specific antibody revealed the presence of active Akt in vehicle treated tumors (**Fig. 2.4h**). Typical cytoplasmic staining with a more intense nuclear pattern was observed while in API-2 and Perifosine treated tumors a significant decrease in phosphor-Akt staining was observed.

Discussion

Previous studies have utilized FRET based reporter molecules for non-invasive imaging of specific kinase activities including PKA[25], PKC[26], and PKB/Akt[27]. Using this platform we here describe the construction of a reporter molecule using the split luciferase technology[22,28]. In the data presented here, inhibition of Akt resulted in activation of bioluminescence activity. Immunoprecipitation of the reporter followed by analysis of phospho-threonine content revealed that the reporter was phosphorylated in an Akt dependent manner. Time and dose dependence of API-2 mediated inhibition of Akt was investigated using the BAR*wt* reporter as well as using traditional western blot analysis. There was a significant correlation between Akt activity status derived from the two methods indicating the quantitative nature of the reporter.

Results shown in **Fig. 2.3** demonstrate that API-2 or Perifosine mediated inhibition of Akt activity resulted in a concominent decrease in the phosphorylation status of the BAR reporter. This validates that the changes in bioluminescence signal from the reporter were due to changes in phosphorylation of the reporter but not to other biological phenomenon within the cells. In addition, these results further validate that the consensus Akt peptide sequence was functional in the context of the BAR*wt* reporter. The Akt substrate peptide sequence used in previous studies[27,29]significantly different from the one described here. In addition, the FRET based reporters developed by Sasaki[29] and Kunkel[27] do not provide for sensitive detection of Akt in live animals. A number of our results strongly suggest that the BAR reporter is specific for Akt. First, the fact that treatment with rapamycin whose target mTOR is downstream of Akt, did not significantly alter BLI activity, while LY294002 which inhibits PI-3K upstreatm of Akt

did alter BLI activity. Secondly, results demonstrate that erlotinib treatment of HCC827 but not an erlotinib resistant cell line (NCI-H1975) resulted in EGFR inhibition and a corresponding change in Akt status was observed by BLI.

The ability to non-invasively and quantitatively image Akt activity within a specific tissue in live animals would significantly enhance our understanding of pharmacokinetics and bioavailability of specific drugs. In addition, this would be a powerful tool to validate drug-target interactions of new compounds. The utility of the BAR reporter in this context is clearly demonstrated in our present studies. For example, results presented in **Fig. 2.4e** suggest that significant API-2 levels are present within the tumor in two hours following IP injection. At 40 mg/kg, inhibitory levels of the compound were detected for up to 24 hours which decreased thereafter. In contrast, when 20 mg/kg was delivered IP, peak inhibition was detected at 12 hours and by 24 hours little inhibitory activity was detected. These non-invasive surrogate measures of Akt function were validated by immunohistochemistry of surgically resected tumors. The above observations provide a unique insight into the pharmacodynamics of API-2. In contrast to API-2 for which published pharmacokinetics data are not available, the pharmacokinetics of Perifosine has been extensively studied. Published data demonstrated that high plasma concentrations of the drug could be detected for as long as seven days post treatment[24]. Results obtained from the BAR reporter studies in live animals confirm this observation since high levels of Akt inhibitory activity (as determined by bioluminescence imaging) was detected within two hours of treatment which remained elevated for seven days (**Fig. 2.4f**). These results provide a unique opportunity to design the optimal dosing and schedule regiments for maximal tumor

control (Akt inhibition) and minimal normal tissue toxicity. In the case of Perifosine, once weekly doses may be sufficient, while in the case of API-2, daily treatment with the drug may be needed for optimal efficacy.

The utility of the BAR reporter in studying upstream signaling events of Akt is also demonstrated in the presented results. For example, stimulation of EGFR could be evaluated using Akt activity as a surrogate (**Fig. 2.1h and 2.1i**). This result indicates that activation of reporter tyrosine kinase in response to a mitogenic signal as well as inhibition in response to specific inhibitors can be non-invasively monitored using BLI (**Fig. 2.4a-d**). Interestingly, stimulation of UMSCC1-BAR*wt* cells with EGF and serum resulted in increased levels of phospho-Akt which was consistent with BLI activity, only EGF treated cells had an increase in phospho-EGFR. The lack of EFGR activation in response to serum treatment suggests that Akt activation could have occurred through alternative pathways such as IGFR activation. Treatment of D54-BAR*wt* cells with Perifosine, an alkyl-phospholipid that interferes with the recruitment of pleckstrin homology (PH) domain-containing proteins to 3-OH phosphorylated phosphatidylinositol containing membranes, resulted in a five-fold induction of BLI activity with a concominant inhibition of Akt (**Fig. 2.2d**). Previous time course data in glial cells showed that the activity of Akt was decreased in response to Perifosine within 4 hours[30] which is in agreement with our results. Careful analysis of the dose response profile of Perifosine mediated Akt inhibition as determined by BLI activity or by western blot analysis reveals that a threshold existed wherein concentration of the drug beyond 40 μM (in cell culture) resulted in a much more significant inhibition of Akt. This lack of a linear dose response may be due to the mechanism of action of Perifosine. Previous studies have suggested

that the presence of the alkyl-phopholipid may interfere with recruitment of PH domain containing proteins to the plasma membrane. The threshold for Akt-inhibition observed may be due to the requirement for optimal doses of Perifosine to be present within the plasma membrane for efficient intercalation into the plasma membrane or for efficient blocking of recruitment of PH domain containing proteins.

Multiple oncogenic pathways mediate their effects through Akt which exemplifies the central role of Akt in cell proliferation and survival. For example, activation of reporter tyrosine kinases (PDGFR and EGFR) as well as loss of PTEN, three common molecular events in cancer, all result in constitutive activation of Akt. To this end, development of Akt-inhibitors for anti-cancer therapy is underway at many pharmaceutical houses as well as in academic labs. Molecular imaging of Akt in cells and live animals would greatly facilitate the process of target validation, dose and schedule optimization as well as for rapid identification of a lead compounds from a library using cell based high throughput screening. The *in vivo* results presented here also indicate that this technology will facilitate the determination of pharmacokinetics and pharmacodynamics of drugs in mice which may or may not be of relevance in humans.

Materials and Methods

Gene construction and DNA plasmids. The gene for the BAR reporter was generated in the mammalian expression vector pEF (Invitrogen, CA). N-terminal firefly Luciferase gene (NLuc)[22] was amplified by polymerase chain reaction (PCR) to encode a SalI restriction site followed a Kozak consensus sequence, and a NotI restriction site at the 3' end. FHA2 was amplified from the Rad53p FHA2 domain with a sense primer containing a NotI site and a reverse primer containing an XbaI site. C-terminal firefly Luciferase gene(C-Luc)[22] was amplified to include a 5' XbaI followed by the Akt substrate sequence, QSRPRSCTWPLPRPEKKK[31] flanked by linker (GGSGG) at each side, and a 3' EcoRI following the terminating codon. BAR*mut1* (T596A) and BAR*mut2* (S590A, S594A, T596A) were constructed using the appropriate primers and the QuickChange kit (Stratagene, CA).

Cell culture and transfection. D54 (human glioma) and DU145 (human prostate cancer) cells were maintained in RPMI (Gibco, MD) supplemented with 10% fetal bovine serum (Gibco, MD) or MEM (Gibco, MD) supplemented with 10% fetal bovine serum (Gibco, MD), respectively. The NSCLC cell lines HCC827 and NCI-H1975 were purchased from American Type Culture Collection (Manassas, VA), and maintained in RPMI supplemented with 10% fetal bovine serum. To construct stable cell lines, the BAR reporter plasmids were stably transfected into cells using Fugene (Roche Diagnostics, CA), and the resulting stable clones were selected using 200 μg/ml G418 (Invitrogen, CA) for D54 cells, 300 μg/ml G418 for DU145 cells, 800 μg/ml G418 for HCC827 cells and 1000 μg/ml G418 for NCI-H1975 cells. Resulting cell lines were isolated and

cultured for further analysis by western blots for determination of expression levels of the recombinant protein.

Antibodies and chemicals. Rabbit polyclonal antibodies to Akt, Phospho-Akt (Ser473), Phospho-EGFR (Y845) and Phospho-threonine specific antibody (9381) were purchased from Cell Signaling Technology (Beverly, MA). Rabbit polyclonal antibodies to EGFR (SC-03) was obtained from Santa Cruz biotechnology (Santa Cruz, CA) Perifosine was purchased from Cayman Chemical (Ann Arbor, MI), API-2 was purchased from Tocris (Ellisville, MO). Luciferin was obtained from Biosynth (Naperville, IL). Erlotinib was provided by OSI Pharmaceuticals (Melville, NY).

Western blot analysis. Cell lysates were prepared in NP40 lysis buffer (1% NP40, 150mM NaCl, 25mM Tris pH 8.0) supplemented with protease inhibitors (Calbiochem, CA) and phosphatase inhibitors (Sigma, MO). Proteins were resolved by SDS/PAGE and analyzed by western blotting using appropriate antibodies. Detection of bound antibody was using horseradish peroxidase-conjugated secondary antibodies and enhanced chemiluminescence (Amersham Pharmacia, Uppsala, Sweden).

Immunoprecipitation. Cell extract (5000 μg) were incubated with the appropriate antibody for 1 hour. Immune complexes were captured using protein G−Sepharose (Amersham Biosciences, NJ), and washed using RIPA buffer for 3 times. The resulting pellet was boiled for 5 mins in sample buffer and resolved by SDS/PAGE.

Cytotoxicity 3-(4,5-Dimethylthiazol-2-yl)-2,5-Diphenyltetrazolium Bromide (MTT) Assay. Cells were seeded in 96-well plates and were treated with 1 μM erlotinib or

vehicle for different times. The assay was performed with a Cell Proliferation kit I (MTT, Roche Diagnostics, IN) according to the manufacturer's instructions. A multiwell scanner was used to measure the absorbance at 570–630 nm dual wavelengths. The vehicle controls were assigned a value of 1.

Immunohistochemistry. Paraffin embedded sections were deparaffinized through xylene and a graded series of ethanol. Endogenous peroxidase activity was quenched by incubation in 2% hydrogen peroxide in methanol for 15 minutes and cleared in PBS for 5 minutes. Antigen retrieval was performed by heating the slides in citrate buffer pH6.0 for 10 minutes in a microwave oven. Non-specific binding was blocked by incubation with 5% normal goat serum in PBS + 0.2% Triton X-100 (blocking serum) for 1 hour at room temperature. Slides were then incubated overnight at 4°C with primary antibody, phosphorylated (Ser473) Akt (from Cell Signaling Technologies; Beverley, MA), at 1:50 dilution in blocking serum. The next day slides were washed 5× for 5 minutes each in PBS + 0.2% Triton X-100 (PBS-T) before addition of secondary antibody. Biotinylated goat anti-rabbit secondary antibody (Vector Laboratories) was added at a 1:200 dilution in PBS-T and incubated for 30 minutes at room temperature. Slides were then washed 5× for 5 minutes each with PBS-T. A Vectastain ABC kit (Vector Laboratories) was used to prepare avidin-biotin complexes for detection of secondary antibody. Antigen localization was enhanced with Ni-DAB and Tris-cobalt followed by counterstaining with Mayer's Hematoxylin.

***In vivo* studies.** Subcutaneous tumors expressing BAR*wt* were established by implanting 8 x 10^6 stably transfected D54-BAR*wt* glioma cells in the mammary fat pad of male

athymic mice (CD-1 nu/nu, Charles River Laboratory, MA). When tumors reached approximately 40-60 mm^3 in volume, bioluminescence imaging was done before treatment as well as at various times after treatment with API-2 (20% DMSO/PBS, i.p.), Perifosine (PBS, oral) or vehicle only.

Bioluminescence imaging. Live cell luminescent imaging was achieved by supplementing D-luciferin (100 μg/ml final concentration) in the growth medium. Photon counts for each condition were acquired 5 minutes post-incubation with D-luciferin using an IVIS imaging system (Xenogen). For *in vivo* bioluminescence, animals were anesthetized using 2% isofluorane/air mixture and given a single i.p. dose of 150 mg/kg luciferin in normal saline. Image acquisition was initiated approximately 12 minutes post luciferin injection. Serial BLI images were acquired prior to treatment and followed every 2 hours until completion of the experiment.

Data analysis. Percent changes in signal intensity were calculated using pretreatment values as baseline and plotted as means ± SEM for each of the groups. Statistical comparisons were made by using the unpaired Student's *t* test with a value of $p< 0.05$ being the cut off for significance.

Figure legends

Figure 2.1 The BAR reporter. (a) The domain structure of the BAR reporter. N-Luc and C-Luc are the animo- and carboxyl- terminal domains of firely luciferase that are fused to the appropriate ends of the reporter. The Aktpep domain constitutes a consensus Akt substrate sequence. On either side of the substrate sequence, flexible linker sequence was included (GGSGG). At the amino- terminal of the Aktpep domain the yeast FHA2 phospho-ser/thr binding domain (reisdues 420 to 582)[26] was included. Three versions of the BAR reporter were developed. The BAR*wt* molecule which contains the wild-type Aktpep sequence, the BAR*mut1* molecule which contains a Thr to Ala substitution at the primary phosphrylation site and BAR*mut2* which has all Ser/Thr within the substrate sequence mutated to Ala.

(b) The proposed mechanism of action for the BAR reporter involves Akt-dependent phosphorylation of the Aktpep domain which results in its interaction with the FHA2 domain. In this form (Akt-ON) the reporter has minimal bioluminescence activity. In the absence of Akt activity, association of the N-Luc and C-Luc domains restores BLI activity.

(c) Expression of the three BAR reporters results in the expected polypeptides. Transient transfection into D54 human glioma cells by western blot analysis using a luciferase specific antibody reveals the expected polypeptides for the luciferase expression vector (61 kDa, pEFluciferase) as well as the appropriate BAR reporter plasmids (84 kDa),

(d) Stable cell lines expressing each of the reporters were treated with the Akt inhibitor, API-2 at 40 μM for 1hour. The change in BLI activity over pretreatment levels was

determined and plated as fold induction. Data were derived from a minimum of five experiments.

(e) Western blot analysis of samples from **Fig. 2.1d** using an antibody specific for phospho-Akt, as well as a total Akt antibody.

(f) DU-145 cells expressing luciferase and each of the BAR reporters were treated with API-2 (40 μM for 1hour) and BLI activity pre- and post-treatment were expressed as fold induction. Data were derived from a minimum of five independent experiments.

(g) Cells from one of the experiments in **Fig. 2.1f** were used for western blot analysis using phospho-Akt and total-Akt antibodies.

(h) UMSCC1 cells expressing BAR*wt* reporter were serum starved overnight, treated with 50 ng/ml EGF or 20% serum and imaged at various times (20 mins, 40 mins and 60 mins). The changes in BLI activity over pre-treated level were expressed as percentage change. Data were derived from five independent experiments.

(i) UMSCC1-BAR*wt* cells stimulated with EGF and serum were analyzed by western blot using phospho-Akt, total Akt, phospho-EGFR, total EGFR and GAPDH antibodies.

Figure 2.2 Time and dose dependent imaging of Akt activity. (a) D54-BAR*wt* stable cells were treated with various doses (2 μM, 8 μM, 20 μM, 40 μM, 80 μM, and 120 μM) of Akt inhibitor, API-2, and BLI activity at various times were analyzed and expressed as fold induction over pre-treatment values. Data were derived from a minimum of five independent experiments.

(b) Cell lysates at 30 minute time point in **Fig. 2.2a** were collected for western blot analysis using phospho-Akt, total Akt and luciferase antibodies.

(c) Western blot analysis of API-2 treated samples using 40 μM at various times (**Fig. 2.2a**) was also performed using phospho-Akt, total Akt, as well as luciferase specific antibodies.

(d) D54-BAR*wt* stable cells were also treated with a lipophilic small molecule PI3K inhibitor, Perifosine. Bioluminescence activity in response to various doses of Perifosine (5 μM, 10 μM, 20 μM, 40 μM, 50 μM, 60 μM) was imaged at various times. The changes in BLI activity were expressed as fold induction over pre-treatment values. Data from a minimum of five independent experiments were analyzed.

(e) Cells treated with various doses of Perifosine for 30 mins (**Fig. 2.2d**) were used for western blot analysis using phospho-Akt, total Akt and luciferase specific antibodies.

Figure 2.3 Phosphorylation and specificity of BAR. (a) D54-BAR*wt* cells pre-treatment and following treatment with API-2 (20 μM and 80 μM) for 30 mins were used to prepare extracts for subsequent analysis. Luciferase specific antibody was used to immunoprecipitate the BAR reporter molecule followed by western blot analysis using a phospho-threonine specific antibody, as well as luciferase specific antibody as control.

(b) Western blot analysis was performed on the extracts from **Fig. 2.3a** using phospho-Akt and total Akt specific antibodies.

(c) The changes in BLI activity in untreated and treated (for 30 mins) D54-BARwt stably expressing cells was determined and expressed as fold induction over pre-treatment values. Data were derived from a minimum of five independent experiments.

(d) D54-BAR*wt* expressing cells treated with 100 nM rapamycin or 50 μM LY294002 were imaged at the 1 hour time point. BLI activity was analyzed and plotted as fold induction over pre-treatment values. Data from 5 independent experiments were analyzed.

(e) Cell lysates were prepared from the cells described in **Fig. 2.3d** and analyzed by western blot using antibodies specific for phospho-Akt, total Akt, phospho-p70S6K and total p70S6K.

Figure 2.4 Biological imaging of Akt. (a) Both HCC827 and NCI-H1975 cells stably expressing the BAR*wt* reporter were treated with 1 μM erlotinib or vehicle control for 3 hrs. The change in BLI activity over pretreatment levels was determined and plotted as fold induction.

(b) Western blot analysis of lysates collected from the cells described in **Fig. 2.4a** was performed using antibodies specific for phospho-EGFR, total EGFR, phosphp-Akt, total Akt, as well as actin specific antibodies.

(c) Cell viability of HCC827-BAR*wt* was determined using the MTT assays after continuous exposure to 1 μM erlotinib or vehicle control for 1, 2, 3 or 4 days. Data were derived from triplicate samples and represent the percentage of cells surviving compared to pre-treatment values.

(d) Cell viability of NCI-H1975-BAR*wt* was determined using the MTT assays after continuous exposure to 1μM erlotinib or vehicle control for 1, 2, 3 or 4 days. Data were derived from triplicate samples and represent the percentage of cells surviving compared to pre-treatment values.

(e) D54-BAR*wt* stable cells were implanted subcutaneously into nude mice. Tumor specific bioluminescence activity was monitored in 4 weeks after implantation when tumors reached about 40-60 mm^3 size. BLI activity pre-treatment and in response to treatment with vehicle control (20% DMSO in PBS) or API-2 (20 mg/kg or 40 mg/kg) was monitored at various times. Fold induction of signal intensity was calculated using

pre-treatment values as baseline and plotted as mean ± SEM for each of the groups. At least five animals were used for each treatment group and each animal had two independent tumors.

(f) Bioluminescence activity in tumor bearing mice pre-treatment and in response to treatment with 30 mg/kg Perifosine was analyzed. BLI activity at various times was used to calculate fold induction and expressed as mean ± SEM for each of the groups, based on pre-treatment levels. At least five animals and two tumors per animal were used for each group.

(g) Tumor bearing animals were treated with vehicle control (20% DMSO in PBS), API-2 (20 mg/kg or 40 mg/kg) or Perifosine (30 mg/kg). Images of representative animals are shown at Pre-treatment (Pre), maximal luciferase signal upon treatment (Max), or Post-treatment (Post).

(h) Tumors of vehicle, API-2 (40 mg/kg) or Perifosine (30 mg/kg) treated animals were sectioned at the 6 hour time point, and immunohistochemical staining on paraffin embedded sections was performed using a phospho-Akt specific antibody.

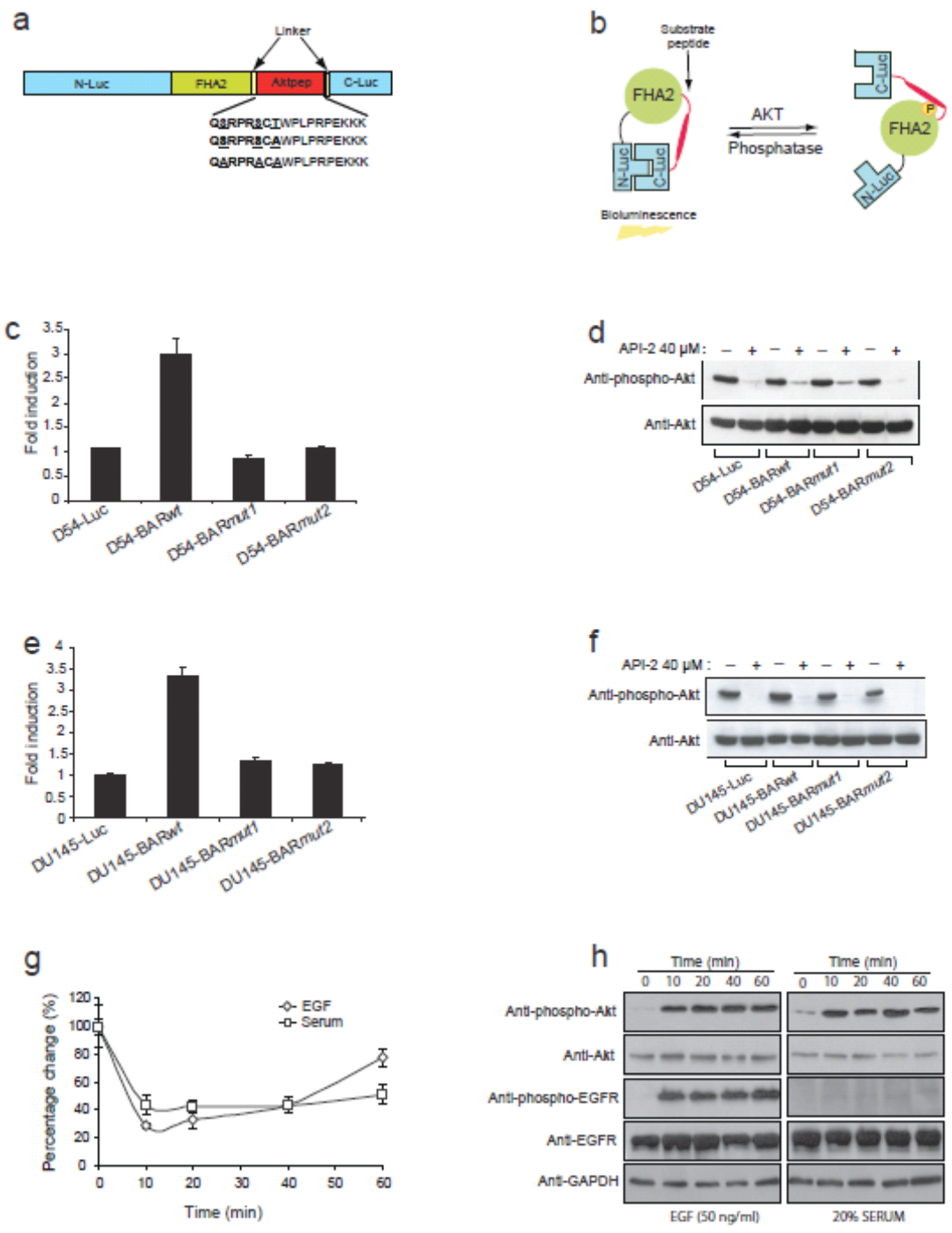
a
Linker
N-Luc
FHA2
Aktpep
C-Luc
QSRPRSCTWPLPRPEKKK
QSRPRSCAWPLPRPEKKK
QARPRACAWPLPRPEKKK
b
Substrate peptide
FHA2
AKT
Phosphatase
C-Luc
N-Luc
P
Bioluminescence
c
Fold induction
D54-Luc
D54-BARwt
D54-BARmut1
D54-BARmut2
d
API-2 40 μM:
Anti-phospho-Akt
Anti-Akt
D54-Luc
D54-BARwt
D54-BARmut1
D54-BARmut2
e
Fold induction
DU145-Luc
DU145-BARwt
DU145-BARmut1
DU145-BARmut2
f
API-2 40 μM:
Anti-phospho-Akt
Anti-Akt
DU145-Luc
DU145-BARwt
DU145-BARmut1
DU145-BARmut2
g
Percentage change (%)
EGF
Serum
Time (min)
h
Time (min)
Anti-phospho-Akt
Anti-Akt
Anti-phospho-EGFR
Anti-EGFR
Anti-GAPDH
EGF (50 ng/ml)
20% SERUM

Figure 2.1

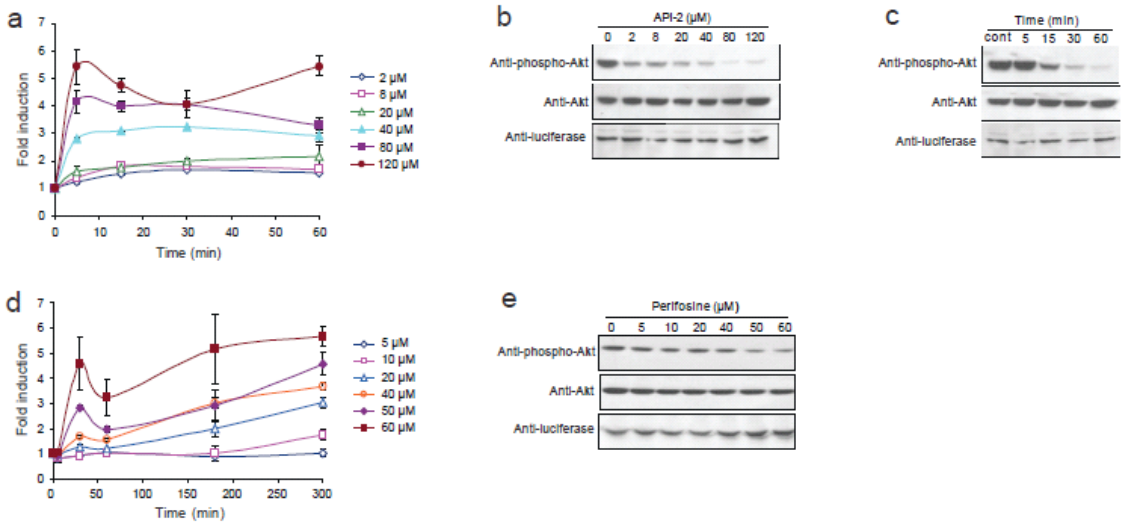
a
Fold induction
Time (min)
2 μM
8 μM
20 μM
40 μM
80 μM
120 μM
b
API-2 (μM)
0 2 8 20 40 80 120
Anti-phospho-Akt
Anti-Akt
Anti-luciferase
c
Time (min)
cont 5 15 30 60
Anti-phospho-Akt
Anti-Akt
Anti-luciferase
d
Fold induction
Time (min)
5 μM
10 μM
20 μM
40 μM
50 μM
60 μM
e
Perifosine (μM)
0 5 10 20 40 50 60
Anti-phospho-Akt
Anti-Akt
Anti-luciferase

Figure 2.2

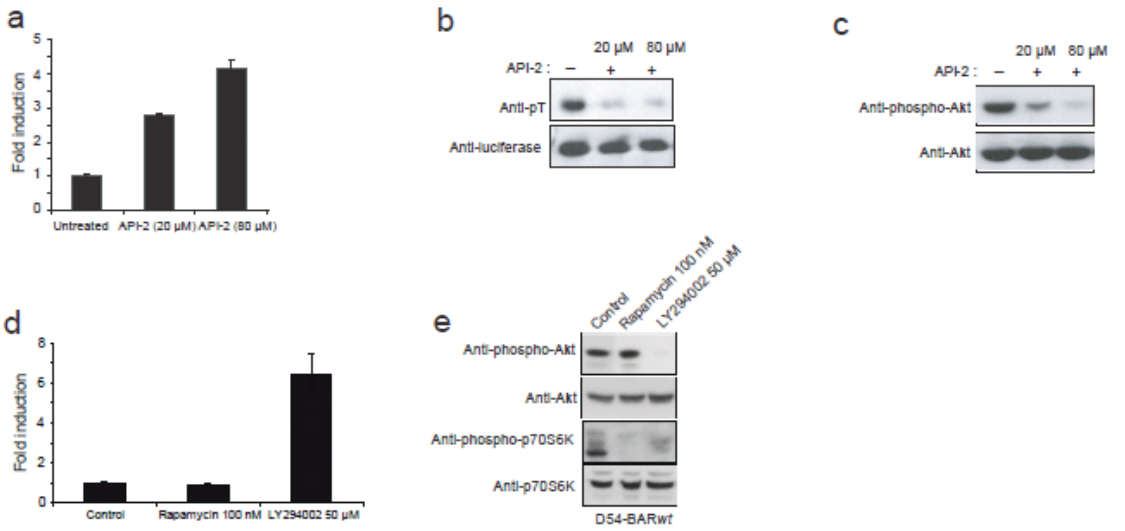
a
Fold induction
Untreated
API-2 (20 μM)
API-2 (80 μM)
b
20 μM 80 μM
API-2 : – + +
Anti-pT
Anti-luciferase
c
20 μM 80 μM
API-2 : – + +
Anti-phospho-Akt
Anti-Akt
d
Fold induction
Control
Rapamycin 100 nM
LY294002 50 μM
e
Control
Rapamycin 100 nM
LY294002 50 μM
Anti-phospho-Akt
Anti-Akt
Anti-phospho-p70S6K
Anti-p70S6K
D54-BARwt

Figure 2.3

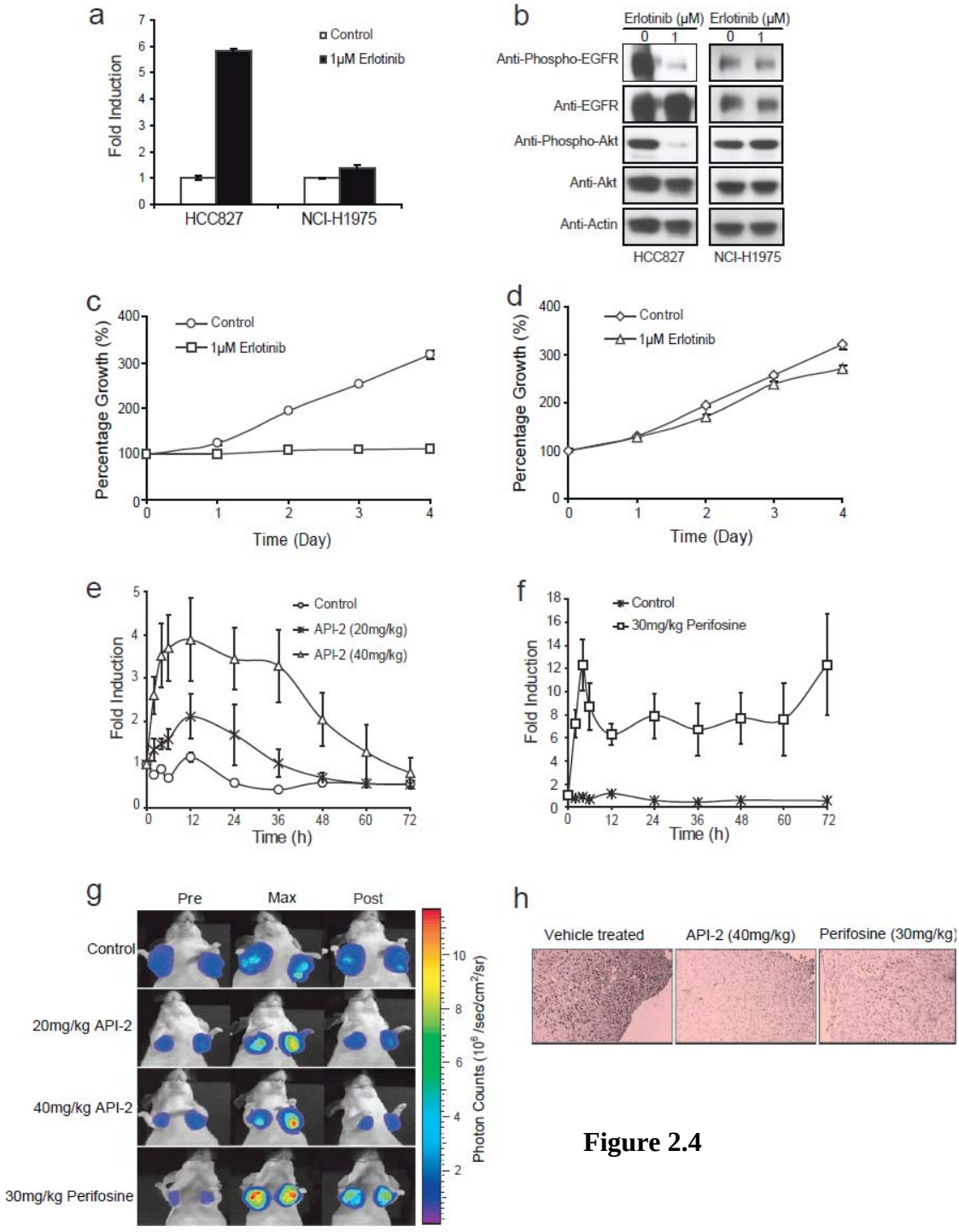
a
Fold Induction
Control
1μM Erlotinib
HCC827
NCI-H1975
b
Erlotinib (μM)
0 1
Erlotinib (μM)
0 1
Anti-Phospho-EGFR
Anti-EGFR
Anti-Phospho-Akt
Anti-Akt
Anti-Actin
HCC827
NCI-H1975
c
Percentage Growth (%)
Control
1μM Erlotinib
Time (Day)
d
Percentage Growth (%)
Control
1μM Erlotinib
Time (Day)
e
Fold Induction
Control
API-2 (20mg/kg)
API-2 (40mg/kg)
Time (h)
f
Fold Induction
Control
30mg/kg Perifosine
Time (h)
g
Pre
Max
Post
Control
20mg/kg API-2
40mg/kg API-2
30mg/kg Perifosine
Photon Counts (10^6 /sec/cm^2/sr)
h
Vehicle treated
API-2 (40mg/kg)
Perifosine (30mg/kg)

Figure 2.4

References

1. Lemmon, M.A. & Schlessinger, J. Regulation of signal transduction and signal diversity by receptor oligomerization. *Trends Biochem Sci* **19**, 459-63 (1994).

2. Romashkova, J.A. & Makarov, S.S. NF-kappaB is a target of AKT in anti-apoptotic PDGF signalling. *Nature* **401**, 86-90 (1999).

3. Brunn, G.J. et al. Direct inhibition of the signaling functions of the mammalian target of rapamycin by the phosphoinositide 3-kinase inhibitors, wortmannin and LY294002. *Embo J* **15**, 5256-67 (1996).

4. Sarbassov, D.D., Guertin, D.A., Ali, S.M. & Sabatini, D.M. Phosphorylation and regulation of Akt/PKB by the rictor-mTOR complex. *Science* **307**, 1098-101 (2005).

5. Brunet, A. et al. Akt promotes cell survival by phosphorylating and inhibiting a Forkhead transcription factor. *Cell* **96**, 857-68 (1999).

6. Zha, J., Harada, H., Yang, E., Jockel, J. & Korsmeyer, S.J. Serine phosphorylation of death agonist BAD in response to survival factor results in binding to 14-3-3 not BCL-X(L). *Cell* **87**, 619-28 (1996).

7. Cross, D.A., Alessi, D.R., Cohen, P., Andjelkovich, M. & Hemmings, B.A. Inhibition of glycogen synthase kinase-3 by insulin mediated by protein kinase B. *Nature* **378**, 785-9 (1995).

8. Mayo, L.D. & Donner, D.B. A phosphatidylinositol 3-kinase/Akt pathway promotes translocation of Mdm2 from the cytoplasm to the nucleus. *Proc Natl Acad Sci U S A* **98**, 11598-603 (2001).

9. Vivanco, I. & Sawyers, C.L. The phosphatidylinositol 3-Kinase AKT pathway in human cancer. *Nat Rev Cancer* **2**, 489-501 (2002).

10. Chen, X. et al. Constitutively active Akt is an important regulator of TRAIL sensitivity in prostate cancer. *Oncogene* **20**, 6073-83 (2001).

11. Hennessy, B.T., Smith, D.L., Ram, P.T., Lu, Y. & Mills, G.B. Exploiting the PI3K/AKT pathway for cancer drug discovery. *Nat Rev Drug Discov* **4**, 988-1004 (2005).

12. Rosenzweig, K.E., Youmell, M.B., Palayoor, S.T. & Price, B.D. Radiosensitization of human tumor cells by the phosphatidylinositol3-kinase inhibitors wortmannin and LY294002 correlates with inhibition of DNA-dependent protein kinase and prolonged G2-M delay. *Clin Cancer Res* **3**, 1149-56 (1997).

13. Hu, L., Zaloudek, C., Mills, G.B., Gray, J. & Jaffe, R.B. In vivo and in vitro ovarian carcinoma growth inhibition by a phosphatidylinositol 3-kinase inhibitor (LY294002). *Clin Cancer Res* **6**, 880-6 (2000).

14. Knight, Z.A. et al. Isoform-specific phosphoinositide 3-kinase inhibitors from an arylmorpholine scaffold. *Bioorg Med Chem* **12**, 4749-59 (2004).

15. DeFeo-Jones, D. et al. Tumor cell sensitization to apoptotic stimuli by selective inhibition of specific Akt/PKB family members. *Mol Cancer Ther* **4**, 271-9 (2005).

16. Kondapaka, S.B., Singh, S.S., Dasmahapatra, G.P., Sausville, E.A. & Roy, K.K. Perifosine, a novel alkylphospholipid, inhibits protein kinase B activation. *Mol Cancer Ther* **2**, 1093-103 (2003).

17. Ouyang, W. et al. PI-3K/Akt pathway-dependent cyclin D1 expression is responsible for arsenite-induced human keratinocyte transformation. *Environ Health Perspect* **116**, 1-6 (2008).

18. Beckmann, N., Mueggler, T., Allegrini, P.R., Laurent, D. & Rudin, M. From anatomy to the target: contributions of magnetic resonance imaging to preclinical pharmaceutical research. *Anat Rec* **265**, 85-100 (2001).

19. Chenevert, T.L. et al. Diffusion magnetic resonance imaging: an early surrogate marker of therapeutic efficacy in brain tumors. *J Natl Cancer Inst* **92**, 2029-36 (2000).

20. Moffat, B.A. et al. Diffusion imaging for evaluation of tumor therapies in preclinical animal models. *Magma* **17**, 249-59 (2004).

21. Durocher, D. & Jackson, S.P. The FHA domain. *FEBS Lett* **513**, 58-66 (2002).

22. Luker, K.E. et al. Kinetics of regulated protein-protein interactions revealed with firefly luciferase complementation imaging in cells and living animals. *Proc Natl Acad Sci U S A* **101**, 12288-93 (2004).

23. Amann, J. et al. Aberrant epidermal growth factor receptor signaling and enhanced sensitivity to EGFR inhibitors in lung cancer. *Cancer Res* **65**, 226-35 (2005).

24. Vink, S.R., Schellens, J.H., van Blitterswijk, W.J. & Verheij, M. Tumor and normal tissue pharmacokinetics of perifosine, an oral anti-cancer alkylphospholipid. *Invest New Drugs* **23**, 279-86 (2005).

25. Zhang, J., Ma, Y., Taylor, S.S. & Tsien, R.Y. Genetically encoded reporters of protein kinase A activity reveal impact of substrate tethering. *Proc Natl Acad Sci U S A* **98**, 14997-5002 (2001).

26. Violin, J.D., Zhang, J., Tsien, R.Y. & Newton, A.C. A genetically encoded fluorescent reporter reveals oscillatory phosphorylation by protein kinase C. *J Cell Biol* **161**, 899-909 (2003).

27. Kunkel, M.T., Ni, Q., Tsien, R.Y., Zhang, J. & Newton, A.C. Spatio-temporal dynamics of protein kinase B/Akt signaling revealed by a genetically encoded fluorescent reporter. *J Biol Chem* **280**, 5581-7 (2005).

28. Ozawa, T., Kaihara, A., Sato, M., Tachihara, K. & Umezawa, Y. Split luciferase as an optical probe for detecting protein-protein interactions in mammalian cells based on protein splicing. *Anal Chem* **73**, 2516-21 (2001).

29. Sasaki, K., Sato, M. & Umezawa, Y. Fluorescent indicators for Akt/protein kinase B and dynamics of Akt activity visualized in living cells. *J Biol Chem* **278**, 30945-51 (2003).

30. Momota, H., Nerio, E. & Holland, E.C. Perifosine inhibits multiple signaling pathways in glial progenitors and cooperates with temozolomide to arrest cell proliferation in gliomas in vivo. *Cancer Res* **65**, 7429-35 (2005).

31. Yaffe, M.B. et al. A motif-based profile scanning approach for genome-wide prediction of signaling pathways. *Nat Biotechnol* **19**, 348-53 (2001).

Chapter 3

Molecular Imaging of c-Met Kinase Activity

Abstract

The receptor tyrosine kinase c-Met and its ligand hepatocyte growth factor/scatter factor (HGF/SF) modulate signaling cascades implicated in cellular migration, invasion, proliferation, survival, and angiogenesis. Consequently, dysregulation of the c-Met/HGF pathway can compromise the cellular capacity to moderate these activities, and lead to cellular proliferation, therapeutic resistance and metastasis in various human malignancies. The therapeutic abrogation of HGF/Met receptor coupling or c-Met receptor-mediated signaling events may provide promising clinical insights into more effective strategies for preventing of tumor growth and spread. In our present study, we constructed a reporter molecule whose bioluminescent activity can be used as surrogate for c-Met tyrosine kinase activity. C-Met activity in cultured cells and tumor xenografts was monitored quantitatively and dynamically in response to the activation or inhibition of the HGF/c-Met signaling pathway via a c-Met kinase inhibitor and an HGF neutralizing antibody. Treatment with the c-Met inhibitor and the HGF neutralizing antibody stimulated the reporter's bioluminescence activity in a dose dependent manner as well as caused rapid regression of U-87 MG tumor xenografts. Results obtained from these studies provide unique insights into the pharmacokinetics and pharmacodynamics

of agents that modulate c-Met activity, validating c-Met as a target for human glioblastoma therapy and reveal the utility of this reporter for developing optimal dosing and schedule parameters for maximal tumor control in cancer treatment.

Introduction

Met receptor tyrosine kinase is a prototypic member of receptor tyrosine kinases and is the only known high-affinity receptor for hepatocyte growth factor (HGF)/ scatter factor (SF)[1]. Met and HGF are widely expressed in a variety of tissues. Met receptor is expressed in epithelial cells, while HGF is secreted by mesenchymal cells and accumulates ubiquitously in tissues[2],[3]. The Met/HGF pathway regulates normal mammalian development that is at the root of abnormalities associated with both Met- and HGF- knockout mice resulted in embryonic expression and epithelial–mesenchymal transition defects during organ morphogenesis[4]. Thus, the Met/HGF signaling pathway plays a critical role in epithelial–mesenchymal interaction and regulation of cell migration, invasion, angiogenesis, and organization of three-dimensional (3D) tubular structures during development and tissue repair[5].

HGF/SF is believed to be a mesenchymal cell-derived cytokine acting for epithelial cells bearing its receptor tyrosine kinase, c-Met. Glioblastoma multiforme (GBM), concomitantly express HGF/SF and c-Met[6]. This finding indicates a presence of autocrine loop of HGF/SF signaling pathway in GBM. The expression of HGF/SF and c-Met is low in low-grade astrocytoma, and c-Met immunoreactivity is correlated with the histological grade of the tumor suggesting that the creation of HGF/SF autocrine loop occurs along with the progression of astrocytic brain tumors.

The role of Met activation in different steps of tumor formation, growth and the invasive phenotype suggests that inhibition of Met may be a valid target for anticancer therapy. Thus the development of surrogate indicators of Met activity which can detect the tumor response to Met inhibition would aid in the development of therapeutic

strategies and enhance our understanding of biological processes of diseases. Moreover, it would facilitate the discovery of lead compounds from a library using cell based high throughput screening.

Molecular imaging has emerged as powerful tools that enable real time and repetitive visualization of gene expression, signal transduction and protein-protein interaction in living subjects. It brings in novel tools for dynamic measurement of signaling cascades and its players for tissue analysis and longitudinal studies of biological processes. Molecular imaging tools have been used to non-invasive real time, dynamic imaging and quantification study of kinase activity[5,7-14]. These tools can aid in preclinical investigations of drug-target interaction and dosage and schedule optimization.

In present study, we developed a split luciferase based reporter to image c-Met kinase activity in live cells and animals. Using this reporter assay, we investigated drug-target interaction and phamacodynamics/pharmacokinetics of c-Met/HGF inhibitors in culture cells as well as in a U87 glioma mouse model. We demonstrated that treatment with an HGF neutralizing antibody in a glioma model induced bioluminescence activity of the reporter as well as led to the delay of tumor growth.

Results

Generation of a bioluminescent Met reporter (BMR) and *in vitro* validation

To detect c-Met kinase activity, we constructed a hybrid molecule (**Fig. 3.1a**) consisting of an 11 amino acid peptide sequence (derived from from Pyk2)[15,16] which is a substrate for c-Met. The BMR reporter also consisted of the *sh2* phospho-tyrosine binding domain (residues 374 to 465)[17], flanked by N-Luc (residues 1 to 416 of firefly luciferase) and C-Luc (residues 398 to 550 of firefly luciferase)[18]. In addition to the wild type reporter, a mutant version as control was also constructed (**Fig. 3.1a**) in which tyrosine (Tyr530) was mutated to alanine (BMR*mut*). The functional basis (**Fig. 3.1b**) of the reporter was that when c-Met was active, phosphorylation of the substrate peptide would result in the binding of the phospho-tyrosine residue to the *sh2* domain, thus preventing reconstitution of N-Luc with C-Luc due to stearic hindrance. Inhibition of c-Met kinase activity would result in loss of phosphorylation of the substrate peptide, thus releasing it from interaction with the *sh2* phospho-tyrosine binding domain. In this situation, N-Luc and C-Luc can associate and reconstitute luciferase activity, which can be detected by bioluminescence imaging. The Met binding domain (MBD)[19] from Gab1 is included to enhance the specificity and sensitivity of the reporter.

To validate BMR as an indicator for Met activity in live cells, stable cell lines using expression vectors for each of the above reporters were constructed. Treatment of U87-BMR*wt* cells with a c-Met inhibitor (SU11274)[20] resulted in a 5 fold induction in bioluminescence activity compare to control. In contrast, U87-BMR*mut* cells had no significant change in bioluminescence activity in response to SU11274 treatment (**Fig. 3.1c**). Western blotting analysis with both stable cell lines upon SU11274 treatment

revealed a decrease in the levels of phospho-c-Met levels, but not total Met levels (**Fig 3.1d**).

To evaluate the ability of BMR to detect changes in C-Met status in response to activation of hepatocyte growth factor (HGF), U87-BMR*wt* cells were serum starved overnight and treated with HGF or epidermal growth factor (EGF) as control. Within 30 min of treatment, cells treated with HGF resulted in a 40% decrease in bioluminescence activity compared to cells treated with vehicle control, which is correlated with an increase in the levels of phospho-c-Met (**Fig. 3.1e**). In contrast, the treatment of EGF did not result in any substantial change in bioluminescence activity as well as in the level of phospho-c-Met (**Fig. 3.1f**). To evaluate the impact of c-Met activity on downstream pathways, we have chosen to focus on PI-3/Akt pathway, which is initiated by many receptor tyrosine kinases including c-Met and EGFR. We constructed a U87 stable cell line expressing bioluminescence Akt reporter (U87-BAR*wt*)[5]. This Akt reporter (BAR*wt*) consists of an Akt consensus peptide and a serine/threonine phosphorylation binding domain (FHA2) flanked by split luciferase molecule. In the presence of Akt kinase activity, phosphorylation of Akt consensus substrate results in the interaction of phosphorylation binding domain, thus preventing reconstitution of the luciferase reporter. In the absence of Akt kinase activity, releasing this steric constrain allows reconstitution of the luciferase reporter molecule, whose activity can be detected noninvasively by bioluminescence imaging. U87-BAR*wt* cells were serum starved overnight and treated with HGF or EGF, and the changes in bioluminescence activity were observed after 30 min. The treatment of both growth factors resulted in a 40% decrease in bioluminescence

activity. Western blot analysis revealed an increase in levels of phosphorylated c-Met with the treatment of both growth factors (**Fig. 3.1g and 3.1h**).

Imaging C-Met activity *in vitro* (maybe a better subtitle)

To evaluate bioluminescent C-Met reporter (BMR) as a quantitative and dynamic surrogate for c-Met activity, U87-BMR*wt* cells were treated with various doses of SU11274 and bioluminescence activity was monitored at different times. In all treatments, bioluminescence activity increased and reached a peak within 15 min and plateaued thereafter (**Fig. 3.2a**). Cells treated with lower doses of SU11274 (1 μM and 2.5 μM) had a very small increase in bioluminescence activity. In contrast, cells treated with higher doses of SU11274 (5 μM, 10 μM and 20 μM) resulted in a much greater increase in bioluminescence activity. Western blotting analysis showed a considerable decrease in the levels of phospho-c-Met of the treatment with higher doses of SU11274 (5 μM, 10 μM and 20 μM) compared to that with lower doses (1 μM and 2.5 μM) of SU11274 (**Fig. 3.2b and 3.2c**), which was consistent with changes in bioluminescence activity.

BMR is a specific indicator for C-Met activity

To further validate whether BMR is phosphorylated in c-Met dependent manner, we treated both U87 cells stably expressing BMR (U87-BMR*wt*) and D54 cells stably expressing BMR (D54-BMR*wt*) with SU11274. The treatment of both cells with SU11274 resulted in ~5 fold induction in bioluminescence activity (**Fig. 3.3a and 3.3c**). Cell extracts were collected from parallel experiments, and BMR molecule was immunoprecipated using a luciferase specific antibody. The immunoprecipitate was resolved using SDS-PAGE and western blotted using a phospho-tyrosine specific antibody as well as a phospho-pyk2 (402) specific antibody. The treatment of SU11274

resulted in a significant decrease in the levels of phospho-tyrosine and phospho-pyk2 (402) in BMR protein which correlated with a decrease in phospho-c-Met levels (**Fig. 3.3b and 3.3d**) and c-Met activity as determined by bioluminescence imaging (**Fig. 3.3a and 3.3c**).

To demonstrate that BMR is a specific indicator for c-Met activity, we used siRNA to knock down c-Met transcripts in U87-BMR*wt* cells and observed bioluminescence activity. SiRNA-mediated targeted downregulation of c-Met expression resulted in a 3 fold induction of the bioluminescence activity compared to scramble SiRNA-transfected U87-BMR*wt* cells (**Fig. 3.3e**). This result was consistent with a substantial decrease in levels of total c-Met and phosphorylated c-Met as determined by western blotting analysis (**Fig. 3.3d**).

C-Met is a target for brain cancer therapy

To investigate the use of BMR in the evaluation of c-Met targeted cancer therapies, U87-BMR*wt* cells were implanted subcutaneously in the flank of nude mice to establish tumors. When tumors reached ~50 mm3, mice were divided randomly into two groups with 8-10 mice per group and treated with control antibody or HGF neutralizing antibody[21] twice a week for 3 weeks. Bioluminescence activity was monitored before and after treatment at various time points. Control antibody treated animals had no significant increase in bioluminescence activity post drug administration. In contrast, in HGF neutralizing antibody treated animals bioluminescence activity increased in 3 h and reached a peak in 5 h (**Fig. 3.4a**). The representative images of mice in each treatment group are shown in **Fig. 3.4b**. To confirm that the differences in bioluminescence activity in these animals are due to changes in c-Met phosphorylation status, the tumors were

collected from HGF neutralizing antibody treated animals at various times and lysed for subsequent analysis. Western blotting analysis revealed the sustained inhibition of c-Met phosphorylation through 12 h after drug administration (**Fig. 3.4c**). Determination of tumor volume showed a remarkable tumor growth delay in HGF neutralizing antibody treated animals compared to control antibody treated animals (**Fig. 3.4e and 3.4f**). By the end of the treatment, tumors of animals treated with control antibody had a mean value of 8 time increase of tumor volume over the tumors before treatment. In contrast, animals treated with HGF neutralizing antibody exhibited a complete growth delay (**Fig. 3.4f**).

Discussion

Molecular imaging tools have provided non- invasive, real time, dynamic and quantitative imaging of kinase activity in living cells and subjects. In the previous study, we have designed a strategy for imaging Akt kinase activity using a luciferase complementation assay. Using this platform, we here described the construction of a reporter molecule to monitor receptor tyrosine kinase c-Met activity. To enhance the specificity of the reporter, the Met Binding Domain (MBD) derived from Gab1 was also included.

Time and dose dependence of SU11274 mediated inhibition of c-Met revealed that bioluminescence activity occurs wherein c-Met is inhibited. In dose dependence studies, doses beyond 5 μM induced greater fold induction of bioluminescence activity which was correlated with substantial reduction of levels of phospho-c-Met detected by western blot analysis. The significant correlation between c-Met activity status derived from both methods indicates the quantitative nature of this reporter. The results from **Fig 3.3** demonstrate that SU11274 mediated inhibition in both U87 and D54 cells resulted in a concominent decrease in the phosphorylation status of the BMR. This validated that changes in the BMR bioluminescence activity was due to changes in phosphorylation status of the reporter. In addition, the data from SiRNA-mediated targeted down-regulation of c-Met expression substantially altered BLI activity. This strongly suggested that the BMR is specific for c-Met.

The ability to non-invasively and quantitatively image c-Met activity within a specific tissue in live animals would significantly enhance our understanding of pharmacokinetics and bioavailability of specific drugs. The utility of the BMR reporter in

validating drug-target interaction and providing information related to the therapeutic effects of agents that modulate this signaling pathway is demonstrated in our present studies. In Fig 4, the treatment of HGF neutralizing antibody showed an increase in bioluminescence activity, and this continuous treatment eventually led to the delay of tumor growth. This validated c-Met as an effective target for brain cancer therapy. The information with regards of schedule and efficacy of therapy would also benefit the potential clinical trials.

We showed that BMR is reversible, allowing monitoring signal propagation as well. For example, activation of c-Met by HGF could be evaluated using BMR as a surrogate (**Fig. 3.1e and 3.1f**). The impact of c-Met on downstream signaling pathway was also demonstrated using a bioluminescent Akt reporter in the presented results (**Fig. 3.1g and 3.1h**). These results indicated that activation of reporter tyrosine kinase as well as its downstream effectors in response to a mitogenic signal can be non-invasively monitored using BLI.

The role of c-Met activation in different stages of tumor development exemplifies c-Met as a valid target for anticancer therapy. To this end, molecular imaging of c-Met activity would aid in the development of therapeutic strategies by providing a platform to investigate target validation, dose and schedule optimization as well as for rapid identification of a lead compounds from a library using cell based high throughput screening.

Materials and Methods

Plasmid construction. The gene for the Bioluminescent MET reporter (BMR*wt*) was generated using our previously described bioluminescent Akt reporter (BAR)[5] as backbone. METpep domain (derived from pyk2, residues 391-411) and the Met binding domain (MBD, residues 486-498 of Gab1) were amplified with the appropriate linkers (GGSGG) using two primers (Primer1: 5'-CGTTGTCTAGAGGAGGAAGTGGAGGACTCTCAGAG AGCTGCAGCATAGAGTCAGACATCTACGCAGAGATTCCCGACGAAACCCTGC GAGGAGGAAGTGG and Primer 2: CGTACCCCGGGTCCTCCACTTCCTCCCCTGAAGCCCATATGAGCAGGAGGAG GAACTTGCATTCCTCCTCCACTTCCTCCTCGCAGGGTTTCGTCGGG) to yield the XbaI-Linker-MET substrate-Linker-MBD-Linker-XmaI coding fragment that was cloned into the Akt reporter as a XbaI-XmaI fragment in place of the Akt substrate peptide. The SH2 domain (derived from mouse shc2, residue 374 to 465) was amplified on a NotI-XbaI fragment using two PCR primers, Primer 1: CCCATAGGCGGCCGCTGGTTCCACGGGAAGC and Primer 2: CGCCTCTAGA CACGGGTTGCTGTAGG. This fragment was cloned into the resulting plasmid (to replace the FHA2 domain). The complete plasmid, SalI-Kozak-Nluc-NotI-SH2-XbaI-Linker-MET substrate-Linker-MBD-Linker-XmaI-Cluc-EcoRI, was generated as a SalI-EcoRI fragment in vector pEF. BMR*mut* (Y530A) was constructed using the appropriate primers and the QuickChange kit (Stratagene, CA).

Cell culture and transfections. D54 (human glioma) and U87 (human glioma) cells were maintained in RPMI (Gibco, MD) supplemented with 10% fetal bovine serum

(Gibco, MD). To construct stable cell lines, bioluminescent Met reporters (BMR*wt* and BMR*mut*) and bioluminescent Akt reporter (BAR*wt*) plasmids were stably transfected into D54 and U87 cells using Lipofectamine 2000 (Invitrogen, CA), and the resulting stable clones were selected using 200 μg/ml G418 (Invitrogen, CA) for D54 cells and 500 μg/ml G418 for U87 cells. Resulting cell lines were isolated and determined by western blots for expression level of the recombinant plasmids.

Antibodies and chemicals. Rabbit polyclonal Met (pYpYpY1230/1234/1235) and mouse polyclonal Met antibodies were purchased from Invitrogen (Carlsbad, CA). Rabbit polyclonal antibodies to Akt, phospho-Akt (Ser473), phospho-EGFR (Y845), phospho-tyrosine and phospho-pyk2 (402) were purchased from Cell Signaling Technology (Beverly, MA). Rabbit EGFR (SC-03) antibody was bought from Santa Cruz biotechnology (Santa Cruz, CA). SU11274 was purchased from Sigma-Aldrich (St. Louis, MO). Luciferin was obtained from Biosynth (Naperville, IL). Hepatocyte growth factors (HGF) were purchased from US Biological (Swampscott, MA); epidermal growth factors (EGF) were purchased from Invitrogen (Carlsbad, CA). HGF neutralizing antibody was a gift from Amgen (Thousand Oaks, CA).

Western blot analysis. Cells were washed with PBS and lysed with NP40 lysis buffer (1% NP40, 150mM NaCl, 25mM Tris pH 8.0) supplemented with protease inhibitors (Calbiochem, CA) and phosphatase inhibitors (Sigma, MO). Proteins were estimated using detergent-compatible protein assay kit from Bio-Rad (Hercules, CA), then resolved by SDS/PAGE and analyzed by western blotting using appropriate antibodies. Detection of bound antibody was using horseradish peroxidase-conjugated secondary antibodies and enhanced chemiluminescence (Amersham Pharmacia, Uppsala, Sweden).

Immunoprecipitation. Immunoprecipitation was done as described[5]. Briefly, cells were washed with PBS and lysed with NP 40 lysis buffer. Cell extracts were incubated with the luciferase specific antibody for 1 hour. Immune complexes were captured using protein G−Sepharose (Amersham Biosciences, NJ), and washed using NP40 lysis buffer for 3 times. The resulting pellet was boiled for 5 minutes in sample buffer and resolved by SDS/PAGE. Protein expression was detected using phospho-tyrosine or phopsho-pyk2 (402) specific antibody followed by horseradish peroxidase-conjugated secondary antibodies and enhanced chemiluminescence.

Small interfering RNA (SiRNA) transfection. U87-BMR*wt* cells were plated onto 6-well plates at a density of 2.5×10^5 cells/ml and incubated for 24 hr in culture medium. The cells were then transfected with Met or scramble siRNAs duplexes using Oligofectamine (Invitrogen) according to the manufacturer suggested protocol. Briefly, Met siRNA or scramble SiRNA (at a final concentration of 50 nM) was added to the mixture of 6 µl of Oligofectamine and 144 µl of OptiMEM medium, and incubated at room temperature for 20 min. The siRNA complex was then dropped onto cells. The medium was replaced 4 h later with fresh complete medium. After 72 h transfection, live cells were imaged for bioluminescence activity and lysed with NP40 lysis buffer for western blotting against total C-Met or phospho-C-Met.

***In vitro* bioluminescence imaging.** Live cell bioluminescence imaging was achieved by supplementing D-luciferin (100 µg/ml final concentration) in the growth medium. Serial BLI images were acquired for each condition 5 minutes post-incubation with D-luciferin using an IVIS imaging system (Xenogen, CA).

***In vivo* studies.** Subcutaneous tumors expressing BMR*wt* were established by implanting 8 x 10^6 stably transfected U87-BMR*wt* glioma cells in the flank of 4 weeks old male athymic mice (CD-1 nu/nu, Charles River Laboratory, MA). When tumors reached approximately 40-60mm^3 in volume, bioluminescence imaging was done before treatment as well as at various times after treatment with HGF neutralizing antibody (i.p. injection) or control antibody (i.p. injection) twice per week for 3 weeks. For the trochar implantation, the tumors were chopped into pieces and washed by growth medium. Tumor pieces of similar size were implanted subcutaneously to flank of male nude mice with a trochar needle.

***In vivo* bioluminescence imaging.** Animals were anesthetized using 2% isofluorane/air mixture and given a single i.p. dose of 150 mg/kg luciferin in normal saline. Image acquisition was initiated approximately 8 minutes post luciferin injection. Serial BLI images were acquired prior to treatment and followed at different times until completion of the experiment.

MR imaging. The imaging was done on a Varian Unity Inova MRI system (company name and location) equipped with 9.4T, 16cm horizontal bore system with a linear rathead coil twice a week, each day after treatment for 3 weeks. During the procedures, animals were anesthetized with 1.25% isoflurane and placed inside the RF coil. Body temperature was maintained by heated air flowing through the coil while imaging. To determine the tumor volume within the cortex, a fast spin echo sequence (TR= 4000ms, TE=40ms) was performed to acquire 15 axial slices with a slice thickness of 1.0 mm, a matrix size of 256X128, and a field of view of 3.0X3.0 cm^2. The volume of each

tumor was calculated based on the number of voxels the tumor occupied in the images using an “in-house” region drawing tool developed in Matlab.

Data analysis. Fold induction in signal intensity was calculated using pretreatment values as baseline and plotted as means ± SEM for each of the groups. Statistical comparisons were made by using the unpaired Student's *t* test with a value of $p < 0.05$ being the cut off for significance.

Figure legends

Figure 3.1. Bioluminescence Met reporter (BMR). a. The domain structure of the BMR. N-Luc and C-Luc are the animo- and carboxyl- terminal domains of firefly luciferase that were fused to animal- and carboxyl- terminal ends of the reporter. METpep domain which constitutes a consensus c-Met substrate sequence was fused to the Met binding domain (MBD). At the animo-terminal of the Met substrate sequence, a tyrosine phosphorylated amino acid residues binding domain (SH2) was added. Flexible linker sequence (GGSGG) was included between SH2 and Metpep, Metpep and MBD as well as MBD and C-Luc. Two versions of the Met reporter were constructed. The BMR*wt* molecule contains the wild-type Metpep sequence, and the BMR*mut* molecule contains a Tyr to Ala substitution at primary phosphrylation site.

b. BMR functions in a manner of c-Met-dependent phosphorylation of the Metpep substrate. In the presence of c-Met (Met-ON), the phosphorylation of Metpep results in its interaction with the SH2 domain, which prevents the binding of split luciferase domains and generates minimal bioluminescence activity. In the absence of c-Met activation (Met-OFF), the reconstitution of N-termial and C-terminal luciferase domains restore the bioluminescent activity.

c. U87-BMR*wt* cells as well as U87-BMR*mut* cells were treated with SU11274 at 5 μM for 1 h. The changes in bioluminescence activity over control vehicle treated levels were determined and plated as fold induction. The data were generated from a minimum of 5 experiments.

d. Cells from one experiment was collected and lysed for western blotting analysis with phospho-Met or total Met specific antibody.

e. U87-BMR*wt* cells were serum starved overnight and treated with 40 ng/ml HGF or 40 ng/ml EGF. The bioluminescence imaging was observed within 30 min of treatment. The changes in bioluminescence activity over pre-treated levels were determined as fold induction.

f. Western blotting analysis of samples from **e** using phospho-Met or total Met specific antibody.

h. U87-BAR*wt* cells were serum starved overnight, treated with 40 ng/ml HGF or 40 ng/ml EGF, and imaged at 30 min. The changes in bioluminescence activity over pre-treated level were determined as fold induction.

i. Cell extracts from **h** were used for western blotting analysis with phospho-Akt as well as total Akt antibody.

Figure 3.2. Imaging of c-Met activity. a. U87-BMR*wt* cells treated with various doses (1, 2.5, 5, 10, and 20 μM) of SU11274 were imaged at different times (5, 15, 30, 60 min). The changes in bioluminescence activity were plotted as fold induction over pretreatment values. Data were derived from a minimum of five independent experiments.

b. Cells treated with SU11274 for 30 min were collected and lysed for western blotting analysis using antibodies specific for phospho-Met or total Met.

c. Western blotting analysis of samples treated with 5 μM SU11274 at various times from **a** were conducted using antibodies specific for phospho-Met or total Met.

Figure 3.3. C-Met dependent phosphorylation of BMR. a. U87-BMR*wt* cells were treated with SU11274 (5 μM) or control vehicle for 1 hr, and changes in bioluminescence activity were plotted as fold induction over control vehicle treatment values.

b. U87-BMR*wt* cells treated with Su11274 (5 μM) or vehicle control were collected and lysed. Luciferase specific antibody was used to immunoprecipitate BMR protein, and western blotting analysis was then performed using phospho-tyrosine, phospho-pyk2 (402) specific antibody, as well as luciferase antibody as control.

c. Cell extracts from **a** were used for western blotting analysis using phospho-Met as well as total Met.

d. D54-BMR*wt* stably transfected cells were treated with SU11274 (5 μM) or control vehicle, and imaged at 24 h time point. Changes in bioluminescence activity were plotted as fold induction using control treatment level as baseline.

e. D54-BMR*wt* cells treated with SU11274 or control vehicle were used to prepare extracts for subsequent analysis. BMR molecule was immunoprecipitate using luciferase antibody and western blotting analysis was conducted using antibodies specific for phospho-tyrosine, phospho-Pyk2 (402) or luciferase as a control.

d. Extracts from **c** were analyzed by western blotting using antibodies specific for phospho-Met and total Met.

Figure 3.4. C-Met as a Target for Brain Cancer Treatment

a. U87-BMR*wt* stably transfected cells were implanted subcutaneously into nude mice. The developed tumors were taken out, chopped into pieces and implanted subcutaneously into male nude mice. When tumor volume reached 50-100 mm3, tumors were separated into two groups. Bioluminescence activity before treatment and in response to treatment with control antibody or HGF neutralizing antibody (300 μg/mouse, ip) was monitored at various times (0, 3, 6, 12 h). Fold induction of signal intensity over pretreatment values

was plotted as mean ± s.e.m. for each of the groups. 8-10 animals were used for each treatment group.

b. Tumor bearing mice were treated with control antibody or HGF neutralizing antibody. Images of representative mice are presented before treatment (Pre) and 6 h after treatment (post).

c. At various time points (0, 3, 6, 12 h) after administration of HGF neutralizing antibody, mice were euthanized, tumor samples were collected and lysates were prepared for western blotting analysis using specific antibodies for phospho-Met and total Met.

d. The lysates from **c** were western blotted using phospho-Met, total Met, phospho-Akt and total Akt.

e. Tumor bearing mice were treated with control antibody or HGF neutralizing antibody (300 μg/mouse, ip) twice per week for three weeks when tumor size reached 50-100 mm3. Tumor volumes obtained form serial MR images of individual mice are displayed versus time. Changes in tumor volume were calculated and expressed as fold induction based on pretreated levels.

f. A series of T2-weighted MR images of a mouse bearing a U87 tumor on the flank before treatment at 2, 6, 14 and 21 days post-treatment, respectively. Each displayed image is from approximately a similar slice within each tumor.

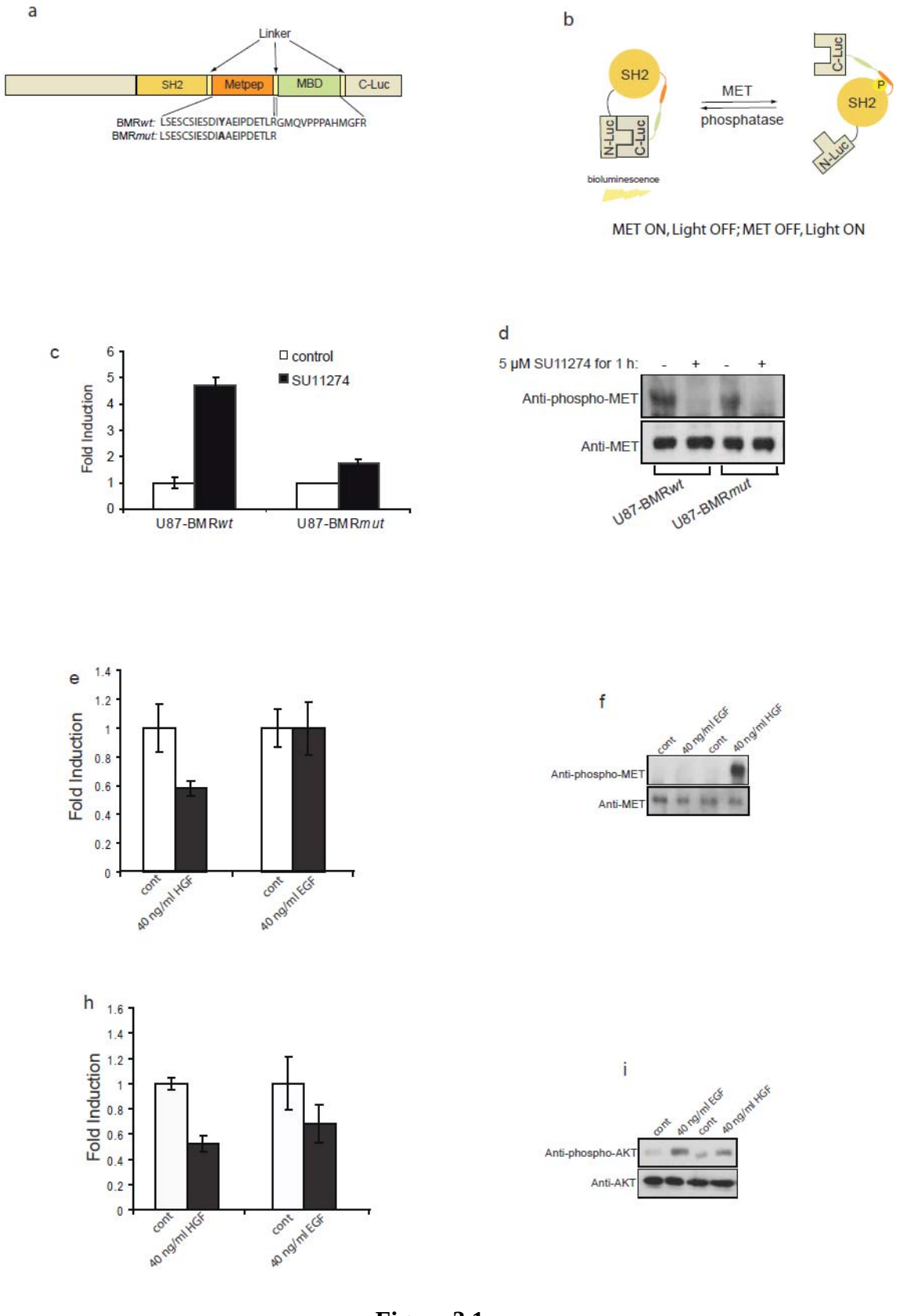
a
Linker
SH2
Metpep
MBD
C-Luc
BMRwt: LSESCSIESDIYAEIPDETLRGMQVPPPAHMGFR
BMRmut: LSESCSIESDIAAEIPDETLR
b
SH2
MET
phosphatase
C-Luc
N-Luc
C-Luc
P
SH2
N-Luc
bioluminescence
MET ON, Light OFF; MET OFF, Light ON
c
control
SU11274
Fold Induction
U87-BMRwt
U87-BMRmut
d
5 μM SU11274 for 1 h:
Anti-phospho-MET
Anti-MET
U87-BMRwt
U87-BMRmut
e
Fold Induction
cont
40 ng/ml HGF
cont
40 ng/ml EGF
f
cont
40 ng/ml EGF
cont
40 ng/ml HGF
Anti-phospho-MET
Anti-MET
h
Fold Induction
cont
40 ng/ml HGF
cont
40 ng/ml EGF
i
cont
40 ng/ml EGF
cont
40 ng/ml HGF
Anti-phospho-AKT
Anti-AKT

Figure 3.1

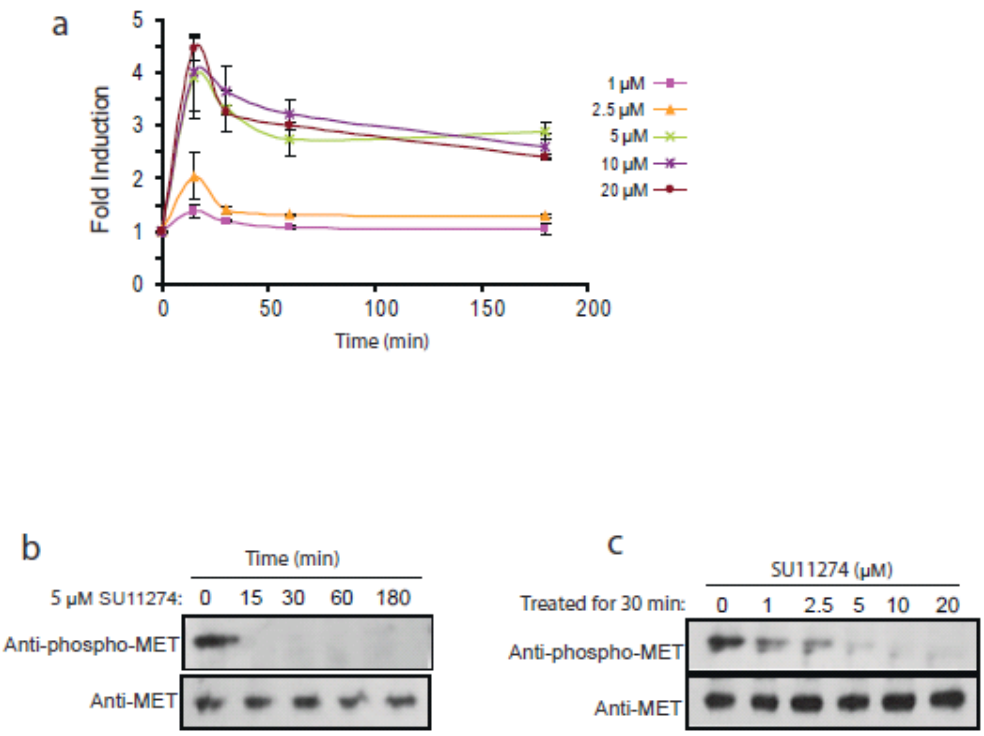
a
Fold Induction
Time (min)
1 μM
2.5 μM
5 μM
10 μM
20 μM
b
Time (min)
5 μM SU11274: 0 15 30 60 180
Anti-phospho-MET
Anti-MET
c
SU11274 (μM)
Treated for 30 min: 0 1 2.5 5 10 20
Anti-phospho-MET
Anti-MET

Figure 3.2

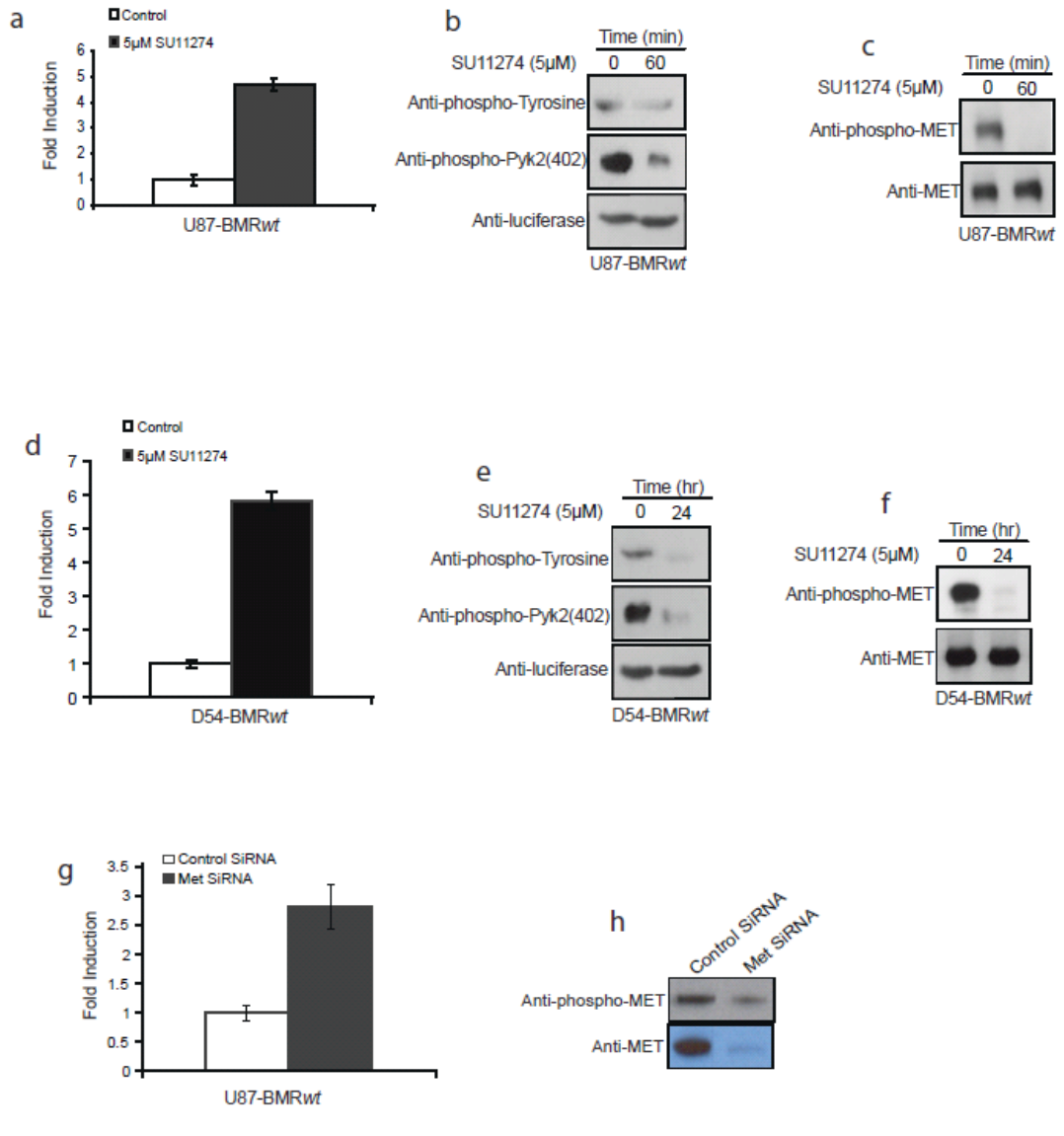
a
Control
5μM SU11274
Fold Induction
U87-BMRwt
b
Time (min)
SU11274 (5μM)
0 60
Anti-phospho-Tyrosine
Anti-phospho-Pyk2(402)
Anti-luciferase
U87-BMRwt
c
Time (min)
SU11274 (5μM)
0 60
Anti-phospho-MET
Anti-MET
U87-BMRwt
d
Control
5μM SU11274
Fold Induction
D54-BMRwt
e
Time (hr)
SU11274 (5μM)
0 24
Anti-phospho-Tyrosine
Anti-phospho-Pyk2(402)
Anti-luciferase
D54-BMRwt
f
Time (hr)
SU11274 (5μM)
0 24
Anti-phospho-MET
Anti-MET
D54-BMRwt
g
Control SiRNA
Met SiRNA
Fold Induction
U87-BMRwt
h
Control SiRNA
Met SiRNA
Anti-phospho-MET
Anti-MET

Figure 3.3

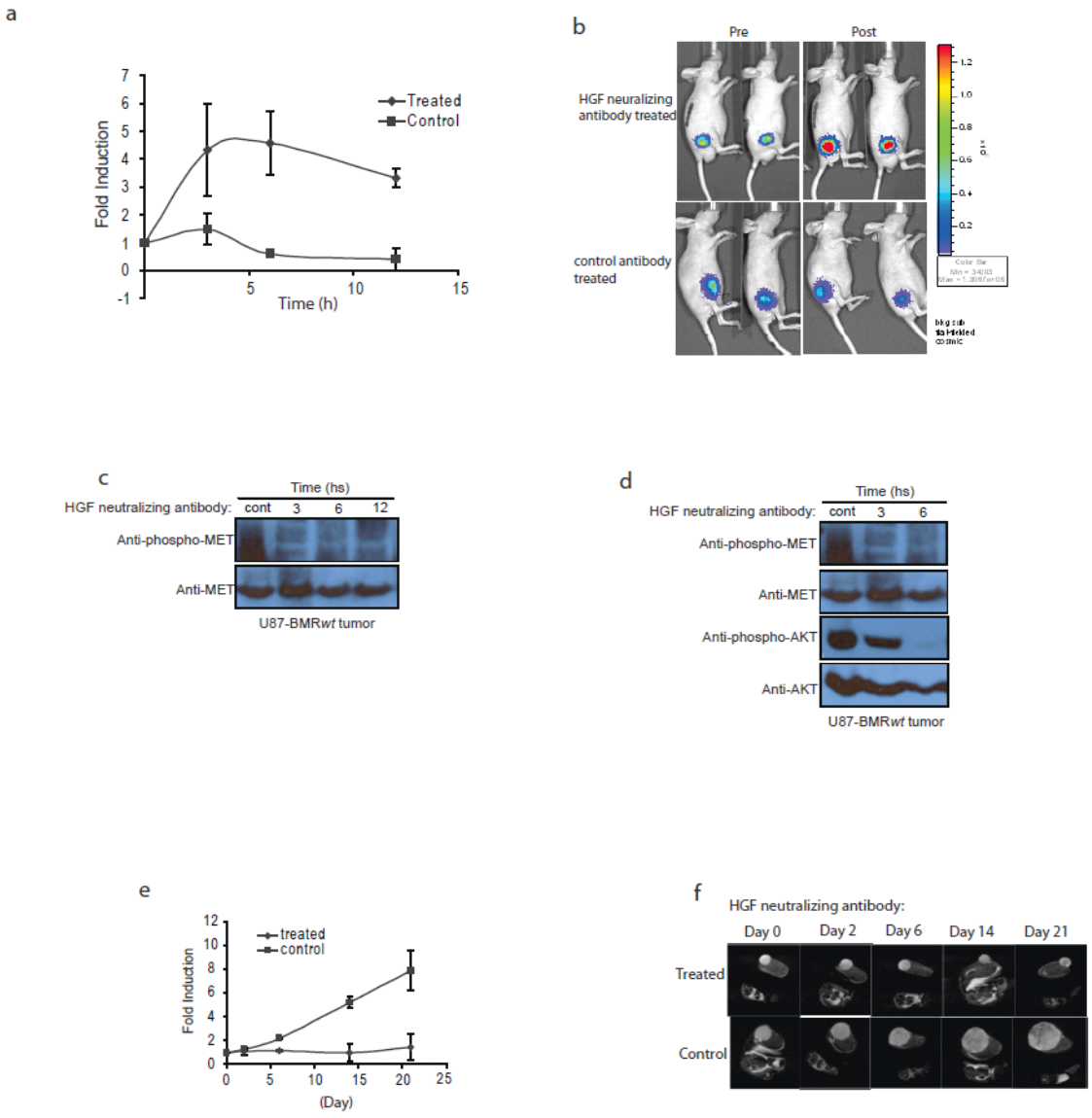
a
Fold Induction
Time (h)
Treated
Control
b
Pre
Post
HGF neuralizing antibody treated
control antibody treated
c
Time (hs)
HGF neutralizing antibody:
cont
3
6
12
Anti-phospho-MET
Anti-MET
U87-BMRwt tumor
d
Time (hs)
HGF neutralizing antibody:
cont
3
6
Anti-phospho-MET
Anti-MET
Anti-phospho-AKT
Anti-AKT
U87-BMRwt tumor
e
Fold Induction
(Day)
treated
control
f
HGF neutralizing antibody:
Day 0
Day 2
Day 6
Day 14
Day 21
Treated
Control

Figure 3.4

References

1. Bottaro, D.P. et al. Identification of the hepatocyte growth factor receptor as the c-met proto-oncogene product. *Science* **251**, 802-4 (1991).

2. Sonnenberg, E., Meyer, D., Weidner, K.M. & Birchmeier, C. Scatter factor/hepatocyte growth factor and its receptor, the c-met tyrosine kinase, can mediate a signal exchange between mesenchyme and epithelia during mouse development. *J Cell Biol* **123**, 223-35 (1993).

3. Tsarfaty, I. et al. The Met proto-oncogene mesenchymal to epithelial cell conversion. *Science* **263**, 98-101 (1994).

4. Bladt, F., Riethmacher, D., Isenmann, S., Aguzzi, A. & Birchmeier, C. Essential role for the c-met receptor in the migration of myogenic precursor cells into the limb bud. *Nature* **376**, 768-71 (1995).

5. Zhang, L. et al. Molecular imaging of Akt kinase activity. *Nat Med* **13**, 1114-9 (2007).

6. Nabeshima, K. et al. Expression of c-Met correlates with grade of malignancy in human astrocytic tumours: an immunohistochemical study. *Histopathology* **31**, 436-43 (1997).

7. Kunkel, M.T., Ni, Q., Tsien, R.Y., Zhang, J. & Newton, A.C. Spatio-temporal dynamics of protein kinase B/Akt signaling revealed by a genetically encoded fluorescent reporter. *J Biol Chem* **280**, 5581-7 (2005).

8. Kunkel, M.T., Toker, A., Tsien, R.Y. & Newton, A.C. Calcium-dependent regulation of protein kinase D revealed by a genetically encoded kinase activity reporter. *J Biol Chem* **282**, 6733-42 (2007).

9. Violin, J.D., Zhang, J., Tsien, R.Y. & Newton, A.C. A genetically encoded fluorescent reporter reveals oscillatory phosphorylation by protein kinase C. *J Cell Biol* **161**, 899-909 (2003).

10. Wang, Y. et al. Visualizing the mechanical activation of Src. *Nature* **434**, 1040-5 (2005).

11. Sasaki, K., Sato, M. & Umezawa, Y. Fluorescent indicators for Akt/protein kinase B and dynamics of Akt activity visualized in living cells. *J Biol Chem* **278**, 30945-51 (2003).

12. Zhang, G.J. et al. Bioluminescent imaging of Cdk2 inhibition in vivo. *Nat Med* **10**, 643-8 (2004).

13. Zhang, L., Bhojani, M.S., Ross, B.D. & Rehemtulla, A. Enhancing Akt imaging through targeted reporter expression. *Mol Imaging* **7**, 168-74 (2008).

14. Zhang, L., Bhojani, M.S., Ross, B.D. & Rehemtulla, A. Molecular imaging of protein kinases. *Cell Cycle* **7**, 314-7 (2008).

15. Maulik, G. et al. Modulation of the c-Met/hepatocyte growth factor pathway in small cell lung cancer. *Clin Cancer Res* **8**, 620-7 (2002).

16. Ma, P.C., Maulik, G., Christensen, J. & Salgia, R. c-Met: structure, functions and potential for therapeutic inhibition. *Cancer Metastasis Rev* **22**, 309-25 (2003).

17. Ting, A.Y., Kain, K.H., Klemke, R.L. & Tsien, R.Y. Genetically encoded fluorescent reporters of protein tyrosine kinase activities in living cells. *Proc Natl Acad Sci U S A* **98**, 15003-8 (2001).

18. Luker, K.E. et al. Kinetics of regulated protein-protein interactions revealed with firefly luciferase complementation imaging in cells and living animals. *Proc Natl Acad Sci U S A* **101**, 12288-93 (2004).

19. Weidner, K.M. et al. Interaction between Gab1 and the c-Met receptor tyrosine kinase is responsible for epithelial morphogenesis. *Nature* **384**, 173-6 (1996).

20. Sattler, M. et al. A novel small molecule met inhibitor induces apoptosis in cells transformed by the oncogenic TPR-MET tyrosine kinase. *Cancer Res* **63**, 5462-9 (2003).

21. Burgess, T. et al. Fully human monoclonal antibodies to hepatocyte growth factor with therapeutic potential against hepatocyte growth factor/c-Met-dependent human tumors. *Cancer Res* **66**, 1721-9 (2006).

Chapter 4

Mouse model for imaging Akt kinase activity

Abstract

The Cre/loxP conditional knockout technology has been used extensively to generate mouse models. Here, we describe the generation of a bioluminescent Akt reporter mouse model wherein Akt kinase activity can be monitored non-invasively in tissues that have undergone Cre-mediated recombination. A *renilla* luciferase gene was included as an internal control in order to standardize Akt reporter activity from one mouse to another. We demonstrated that both bioluminescent Akt reporter and renilla luciferase can be switched on in a Cre-dependent manner in cells or tissues under analysis. Based on these results, we propose that this mouse model can be combined with existing Cre-mediated mouse model, and enable the non-invasive and longitudinal study of tumor growth and therapeutic response using bioluminescence imaging.

Introduction

Cre is a Type I topoisomerase bacteriophage P1 which mediates site-specific recombination of DNA between pairs of loxP sites. LoxP is a 34 bp DNA sequence at which Cre catalyzes site-specific DNA recombination[1]. Cre/loxP dependent recombination allows spatial and temporal gene knockout in mice[2]. The application of Cre/loxP technology has resulted in a new generation of conditional mouse cancer models and it has been proved as the most useful tool to study tumor etiology *in vivo*[3]. Using this system, the disease can be investigated in mice in a more clinical relevant way to facilitate the understanding of complex signaling cascades. It also possesses the potential to evaluate or develop novel targeted therapies.

Protein kinase Akt is deregulated in many human cancers, and it is considered as a key determinant of tumor progression[4-7]. Mouse cancer models based on conditional regulation of Akt or its mediators have been developed and used successfully to study cancer biology in an *in vivo* setting[8-12]. However, non-visible nature of tumorigenesis has limited its application. Moreover, as histology analysis is the most efficient way to evaluate the treatment, longitudinal studies of biological processes and tumor response to therapies have become problematic.

Noninvasive bioluminescence imaging has emerged as a powerful tool to study signaling cascades and follow tumor progression in living subjects. This methodology allows non-invasive and real time imaging tumor at deep-tissue sites in mice. It is also suited for drug discovery research in animal disease models *in vivo*[13-16]. In our previous study, we have constructed a bioluminescence Akt reporter which reports on Akt kinase activity in a xenografted mouse model[17]. We now generated a ubiquitously expressing

Cre-mediated conditional bioluminescent Akt reporter mouse model. This mouse model can be used to generate a range of Cre-mediated mouse cancer models by combining with existing Cre/loxP conditional knockout mouse models, and enable imaging the role of Akt in tumoregenesis and in response to cancer therapies.

Results

Construction of bioluminescent Akt reporter transgene

To generate a conditional mouse model wherein serine/threonine Akt kinase activity can be non-invasively detected, we generated a transgenic mouse model expressing Cre-dependent bioluminescent Akt reporter construct (AktR*loxploxp*) as described in **Fig. 4.1**. Briefly, the EF constitutive promoter drives transcription of the *tomato* coding sequence[18]. The presence of a transcription stop site and poly-adenylation target site (poly-A) at the end of the *tomato* coding sequence results in the termination of transcription after *tomato* therefore prevent bioluminescent Akt reporter expression. In the Cre-dependent matter, recombination of the *loxp* sequences results in the deletion of the tomato coding sequence as well as the poly-A sequences. The promoter then drives the expression of bioluminescent Akt reporter which is based on firefly luciferase as well as the IRES (internal ribosome entry site) and the *renilla* luciferase (*r*luc). The expression of renilla luciferase serves as internal control for the number of cells that express bioluminescent Akt reporter so that we can standardize Akt reporter activity from one mouse to another.

In vitro validation of AktR*loxploxp* gene

The AktR*loxploxp* plasmid was transiently transfected to 293T cells. 2 days after transfection, the cells were treated with or without adenovirus expressing Cre recombinase (AdCre). Cells treated with AdCre showed a significant decrease of the expression of tomato protein compared to untreated cells (**Fig. 4.2a**). Bioluminescence activity for bioluminescent Akt reporter as well as renilla luciferase was then observed. The AdCre treated cells resulted in a substantial increase in the expression of Akt reporter

as well as renilla luciferase. In contrast, untreated cells showed no expression of both proteins (**Fig. 4.2b and 4.2c**).

Cre dependent expression of Akt reporter in AktR*loxploxp* mouse

The AktR*loxploxp* construct was microinjected into fertilized FVB/N oocytes, and the mice carrying transgene were selected as founders and bred with wide type FVB/N to generate AktR*loxploxp* expressing mouse. To validate if the Akt reporter can be switched on in a Cre dependent manner, we intrabursally injected adenovirus expressing Cre recombinase (AdCre) into the right ovarian bursal cavity of a AktR*loxploxp* gene positive mouse as well as a AktR*loxploxp* gene negative mouse as control. 72 h after virus injection, both mice were imaged. AktR*loxploxp* positive mouse showed a substantial increase of bioluminescence activity at the position of right ovary but not other parts of the body, while AktR*loxploxp* negative mouse showed no bioluminescence activity (**Fig. 4.3**).

Discussion

Molecular imaging provides the tools for quantitative, dynamic and real time monitoring specific signaling pathways in a living subject. The ability to introduce molecular imaging technology to conditional mouse models would allow noninvasive and longitudinal studies of dynamic biological processes. In our previous studies, we have developed a split firefly luciferase based reporter (BAR) wherein Akt activity can be detected by bioluminescence imaging[17]. We showed that the inhibition of Akt activity using various kinase inhibitors resulted in an increase of bioluminescence activity in a xenografted mouse model, which indicated that BAR was a surrogate for Akt activity in terms of quantity and dynamics. In the present study, we generated conditional mouse model expressing bioluminescent Akt reporter to non-invasively monitor Akt in tissues that have undergone Cre-mediated recombination. To compare one mouse to another, we include a *renilla* luciferase gene as an internal control. Using this mouse model we could study signaling cascades related to cancer or any environmental stimulation which regulates Akt activity in a tissue specific manner. For such purpose, this mouse model can be combined with existing Cre-mediated mouse models.

The ability to non-invasively imaging Akt activity in a conditional cancer mouse model will facilitate our understanding of complex molecular mechanisms in representative tumor model system. It will also enhance our capacity to design the most rational and successful method for cancer therapies in future clinical trials. Furthermore, this model system can be used to discover novel compounds targeting PI-3K/Akt pathway which plays a major role in cancers.

Materials and Methods

Gene construction and DNA plasmids. The plasmid for bioluminescent Akt reporter transgenic mouse (AktR*loxploxp*) was generated in the mammalian expression vector pEF (Invitrogen, CA). The *tomato* gene was amplified by polymerase chain reaction (PCR) to encode a SalI restriction site followed a loxp sequence, and a SalI restriction site following a poly-A tail and a loxp sequence at the 3' end. Akt reporter (BAR)[17] was amplified with a sense primer containing a SalI site and a reverse primer containing an EcoRI site. The IRES-renilla luciferase fragment was amplified to include a 5' EcoRI site and a 3' SpeI. The complete plasmid was ligated and inserted into the pEF vector.

AktR*loxploxp* transgenic mice. The *AktRloxploxp* transgenic mice were generated by pronuclear microinjection of the gene into fertilized FVB/N (Charles River, Wilmington MA) oocytes. The genotype of each strain was confirmed by PCR using tail biopsy DNA. Quantitative PCR was performed to select homozygotes of strain. All animal procedures were approved by the University of Michigan's Committee on Use and Care of Animals.

Cell culture and transfection. 293T cells were maintained in DMEM with 10% fetal bovine serum, 1% L-glutamine, 100 μg/ml penicillin, 100 μg/ml streptomycin. Transfection using Fugene 6 (Roche Diagnostics, Indianapolic, IN) was carried out according to the manufacturer's instructions.

Bioluminescence imaging. Live cell luminescent imaging for firefly luciferase was achieved by supplementing D-luciferin in the growth medium. Photon counts for each condition were acquired 5 minutes post-incubation with D-luciferin using an IVIS imaging system (Xenogen). Renilla luciferase imaging in living cells was acquired right after the addition of coelenterazine using an IVIS imaging system. For in vivo

bioluminescence, animals were anesthetized using 2% isofluorane/air mixture and given a single i.p. dose of 150 mg/kg luciferin in normal saline. Image acquisition was initiated approximately 12 minutes post luciferin injection.

Figure legends

Figure 4.1 Construction of bioluminescent Akt reporter transgenic mouse (AktR*loxploxp*). The transgenic mouse model was generated using expression cassette shown here. EF constitutive promoter drives gene transcription. In the absence of Cre, transcription terminates at poly-adenylation (poly-A) sequence following the tomato sequence thus preventing the expression of bioluminescent Akt reporter. In the presence of Cre, the recombination of the *loxp* sequences results in the deletion of the tomato coding sequence as well as the poly-A sequence therefore the EF promoter drives the expression of bioluminescent Akt reporter as well as *renilla* luciferase.

Figure 4.2 *In vitro* validation. The AktR*loxploxp* plasmid was transiently transfected into 293T cells. Within 30 h after transfection, cells were treated with control vehicle or adenovirus expressing Cre recombines. Fluorescent and bioluminescent activities were measured within 12 h after the treatment. FL: firefly luciferase; RL: renilla luciferase.

Figure 4.3 Cre dependent expression of Akt reporter in AktR*loxploxp* mouse. 6 week old AktR*loxploxp* gene positive mouse and AktR*loxploxp* gene negative mouse were intrabursally delivered adenovirus expressing Cre recombinase (AdCre) into the right ovarian bursal cavity. 72 h after virus injection, mice were imaged for bioluminescence activity.

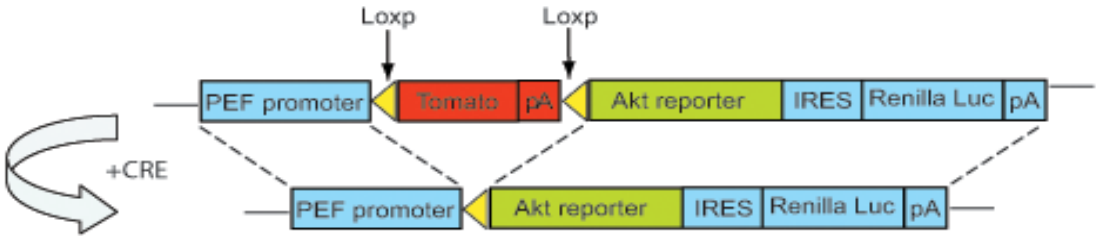
Loxp
Loxp
PEF promoter
Tomato
pA
Akt reporter
IRES
Renilla Luc
pA
+CRE
PEF promoter
Akt reporter
IRES
Renilla Luc
pA

Figure 4.1

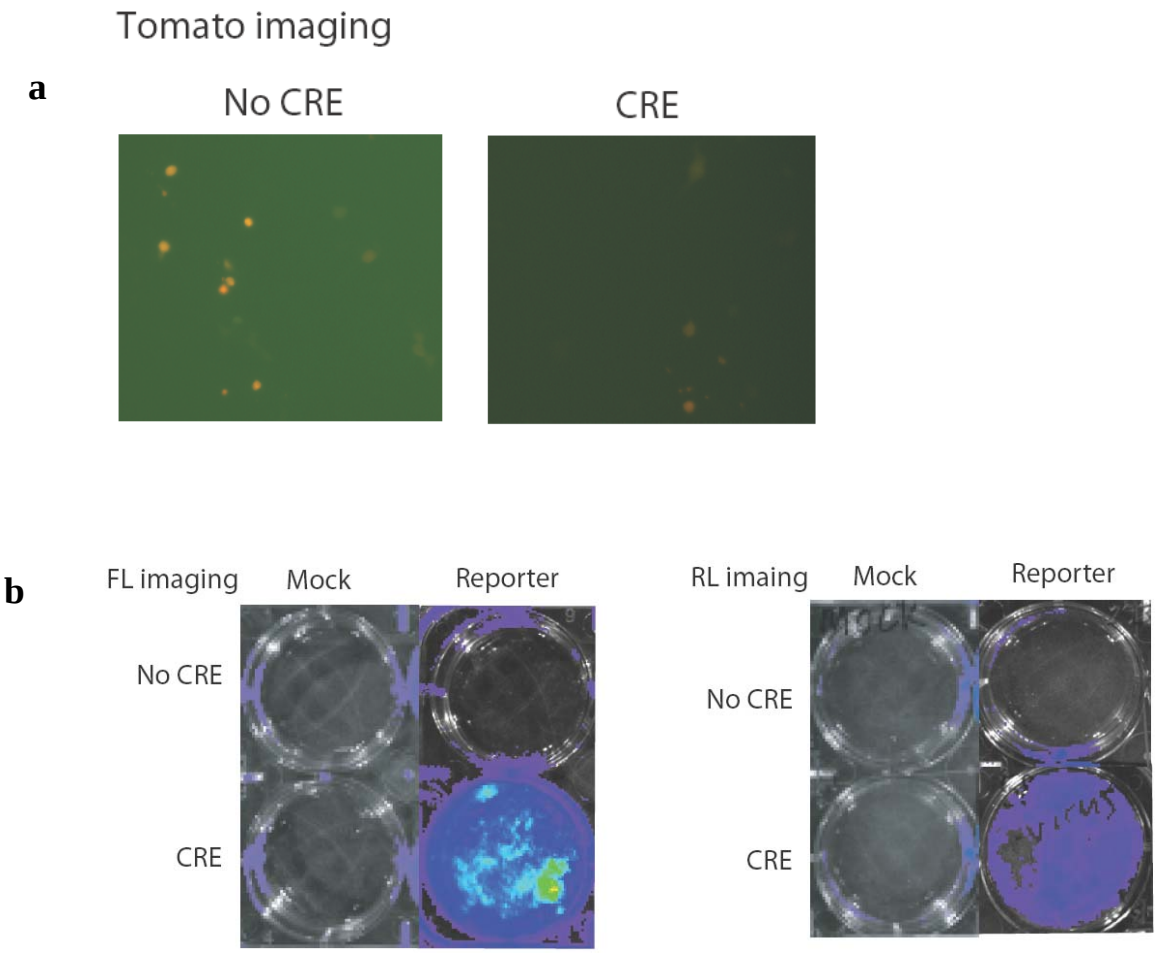
a
Tomato imaging
No CRE
CRE
b
FL imaging
Mock
Reporter
No CRE
CRE
RL imaing
Mock
Reporter
No CRE
CRE

Figure 4.2

+ -

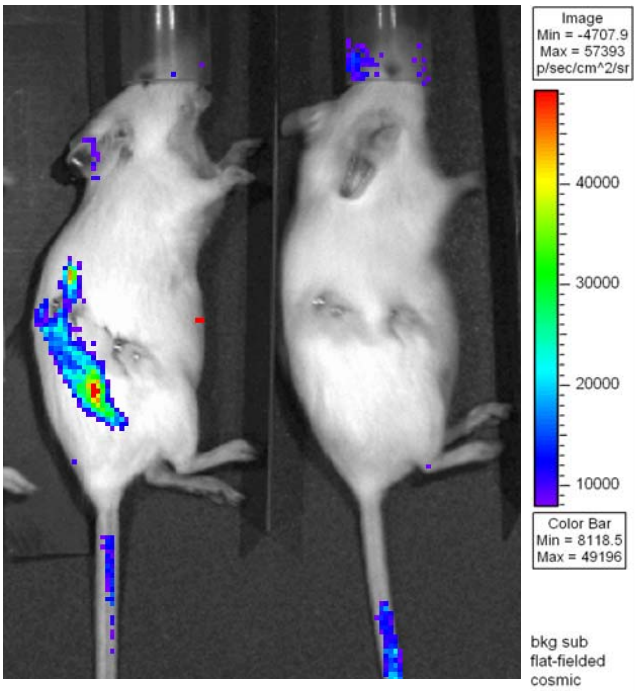
Image
Min = -4707.9
Max = 57393
p/sec/cm^2/sr
40000
30000
20000
10000
Color Bar
Min = 8118.5
Max = 49196
bkg sub
flat-fielded
cosmic

Figure 4.3

References

1. Hoess, R.H. & Abremski, K. Mechanism of strand cleavage and exchange in the Cre-lox site-specific recombination system. *J Mol Biol* **181**, 351-62 (1985).

2. Nagy, A. Cre recombinase: the universal reagent for genome tailoring. *Genesis* **26**, 99-109 (2000).

3. Jonkers, J. & Berns, A. Conditional mouse models of sporadic cancer. *Nat Rev Cancer* **2**, 251-65 (2002).

4. Cheng, J.Q. et al. Amplification of AKT2 in human pancreatic cells and inhibition of AKT2 expression and tumorigenicity by antisense RNA. *Proc Natl Acad Sci U S A* **93**, 3636-41 (1996).

5. Ruggeri, B.A., Huang, L., Wood, M., Cheng, J.Q. & Testa, J.R. Amplification and overexpression of the AKT2 oncogene in a subset of human pancreatic ductal adenocarcinomas. *Mol Carcinog* **21**, 81-6 (1998).

6. Bellacosa, A. et al. Molecular alterations of the AKT2 oncogene in ovarian and breast carcinomas. *Int J Cancer* **64**, 280-5 (1995).

7. Staal, S.P. Molecular cloning of the akt oncogene and its human homologues AKT1 and AKT2: amplification of AKT1 in a primary human gastric adenocarcinoma. *Proc Natl Acad Sci U S A* **84**, 5034-7 (1987).

8. Baba, M. et al. Kidney-targeted Birt-Hogg-Dube gene inactivation in a mouse model: Erk1/2 and Akt-mTOR activation, cell hyperproliferation, and polycystic kidneys. *J Natl Cancer Inst* **100**, 140-54 (2008).

9. Daikoku, T. et al. Conditional loss of uterine Pten unfailingly and rapidly induces endometrial cancer in mice. *Cancer Res* **68**, 5619-27 (2008).

10. Lague, M.N. et al. Synergistic effects of Pten loss and WNT/CTNNB1 signaling pathway activation in ovarian granulosa cell tumor development and progression. *Carcinogenesis* **29**, 2062-72 (2008).

11. Ma, X. et al. Targeted biallelic inactivation of Pten in the mouse prostate leads to prostate cancer accompanied by increased epithelial cell proliferation but not by reduced apoptosis. *Cancer Res* **65**, 5730-9 (2005).

12. Chen, C.S. et al. NF-kappaB-activated tissue transglutaminase is involved in ethanol-induced hepatic injury and the possible role of propolis in preventing fibrogenesis. *Toxicology* **246**, 148-57 (2008).

13. Beckmann, N., Mueggler, T., Allegrini, P.R., Laurent, D. & Rudin, M. From anatomy to the target: contributions of magnetic resonance imaging to preclinical pharmaceutical research. *Anat Rec* **265**, 85-100 (2001).

14. Chenevert, T.L. et al. Diffusion magnetic resonance imaging: an early surrogate marker of therapeutic efficacy in brain tumors. *J Natl Cancer Inst* **92**, 2029-36 (2000).

15. Moffat, B.A. et al. Diffusion imaging for evaluation of tumor therapies in preclinical animal models. *Magma* **17**, 249-59 (2004).

16. Morgan, B., Horsfield, M.A. & Steward, W.P. The role of imaging in the clinical development of antiangiogenic agents. *Hematol Oncol Clin North Am* **18**, 1183-206, x (2004).

17. Zhang, L. et al. Molecular imaging of Akt kinase activity. *Nat Med* **13**, 1114-9 (2007).

18. Shaner, N.C. et al. Improved monomeric red, orange and yellow fluorescent proteins derived from Discosoma sp. red fluorescent protein. *Nat Biotechnol* **22**, 1567-72 (2004).

Chapter 5

Conclusion and Outlook

Protein kinases are involved in every step of mammalian development. Consequently, aberrant activation of protein kinases can cause deleterious effects. The elucidation of protein kinase activity will contribute to a better understanding of the signal transduction cascades, as well as the development of novel therapeutic agents. To non-invasive, real time, quantitatively and dynamically investigate protein kinase activity, bioluminescence reporter assays were designed in this work. Such reporter assays were used to study serine/threonine kinase Akt and receptor tyrosine kinase Met in response to inhibition as well as activation of kinase activity in cultured cells and tumor xenografts. To investigate protein kinase activity in a tissue dependent manner, a Cre-mediated transgenic mouse model expressing bioluminescent Akt reporter was generated.

Bioluminescent Akt reporter

In chapter 2, a bioluminescent Akt reporter was constructed to monitor serine/threonine kinase Akt activity in cultured cells and in tumor xenografts. Akt is a signaling hub wherein many upstream signaling pathways converge. Through phosphorylation of downstream events, it regulates cellular growth, survival and proliferation. Upregulation of Akt is observed in 60% of human malignancies, and involved in tumor initiation, progression, and resistance to cancer treatment[1,2]. Akt has

been studied for decades and numerous compounds have been developed to target Akt even though many of them failed clinical trials because of organ toxicity[3,4].

Using this reporter assay, one could identify compounds from synthetic and natural compound libraries that pass the barriers of solubility, membrane permeability and toxicity, thus enhancing their chance of being successful in experimental and clinical validation. This reporter assay enables one to determine pharmacokinetics and pharmacodynamics of leading compounds. To be eventually approved for clinical use, a candidate must possess suitable pharmokinetic properties, such as remaining activity when reaching the target organs and non-toxic to metabolic organs. Current toxicological evaluation of novel drug candidates in cancer has traditionally involved identification of the Maximum Tolerated Dose (MTD) using dose escalation studies (in humans and in animal models). At doses below the MTD, additional toxicological studies are conducted to detect asymptomatic toxicity in various organ systems (in animal models). Subsequently, the efficacy of the drug is evaluated at "safe" doses using tumor volume and survival as endpoints. This reporter assay provides a unique opportunity to streamline this cumbersome, time consuming and expensive process. Using this reporter assay, one can in a single cohort determine if (1) Is the drug hitting the target? (2) Does this drug-target interaction have the desired effect? (3) Efficacy can be evaluated more specifically and in an individualized manner. Knowing this information early *in vivo* will speed up drug development (Identification of efficacious and non-toxic doses/schedule is streamlined), terminate the development of compounds early if they do not possess the desired mechanism ("dirty" compounds that have efficacy through off-target effects often end up having toxicological implications), and facilitate *in vivo* target validation

(provides confirmation that the intended target is a key in the transformed phenotype for that disease).

Bioluminescent reporter functions as 'kinase on, light off; kinase off, light on', so that it is a "gain of function assay" compared to traditional biochemical assays when used for high throughput screening of compound libraries. For example, compounds that are cytotoxic and thus result in loss of signal would not show up as false positives using the bioluminescence reporter platform. Such assay would narrow down the number of hits to a smaller group of "true positives".

This reporter assay can also be utilized to study the role of protein kinases in other disease model systems. For example, one can use this reporter assay to study toxins induced cytotoxicity or organ injury at cellular and molecular levels. It has been reported by several groups that PI-3/Akt signaling pathway can be activated by environmental toxins such as arsenite or cadmium[5-10]. For example, published data showed that PI-3K/Akt pathway is responsible for arsenite-induced human skin carcinogenic effect. The elevation of Akt phospho-levels in response to arsenite treatment was detected using western blotting analysis. However, this method was invasive, time consuming and only detected Akt activity at a specific time. In contrast, Akt reporter assay would take much shorter time and provide a dynamic and quantitative observation of Akt status. In addition, one can use Akt reporter assay to monitor Akt activation in response to arsenite in a mouse model, and observe the following human skin carcinogenic effect in the same mouse. Therefore, Akt reporter assay allows the identification of signaling molecule pathways involved in toxins-induced cellular alterations and facilitates the investigation of the carcinogenic effect of toxins in a natural and convenient way.

The specificity for bioluminescence reporter strategy is also dependent on its subcellular localization. For example, activation of Akt requires membrane translocation by PI-3 kinase-generated D3-phosphorylated phosphoinositides, PIP3. Based on the fact that Akt is recruited to the plasma membrane upon activation, we constructed a membrane-targeted bioluminescent Akt reporter by fusing 10 amino-terminal residues of Lyn kinase responsible for myristoylation and palmitoylation to BAR. The data validated that membrane-targeted Akt reporter confers the increased sensitivity in reporting Akt activity[11]. Thus, reporters which are co-localized with activated kinases in the subcellular location would result in increased reporter activity. Bioluminescent kinase reporter assay can also be adapted for other protein kinases using suitable substrates and phosphorylation recognition domains.

In chapter 4, a Cre-mediated bioluminescent Akt reporter mouse model was generated to enable non-invasive imaging of Akt activity in tissues that have undergone Cre-mediated recombination. Using this mouse model, one can study signaling cascades which regulate Akt activity in a tissue specific manner. For future study, this mouse model can be combined with existing Cre-mediated mouse models that spontaneously develop tumors, therefore provide a system which is more clinical relevance. Using such model, one can study the role of Akt in tumoregenesis, Akt status in response to cancer therapies, and identify targeted therapies which inhibit Akt most efficiently for efficacy.

Bioluminescent Met reporter

In chapter 3, a bioluminescent Met reporter was developed to monitor receptor tyrosine kinase Met activity quantitatively and dynamically in response to inhibition or activation *in vitro* and *in vivo*. Treatment with an HGF neutralizing antibody in a glioma

model induced bioluminescence activity of the reporter as well as led to rapid regression of tumor xenografts. It further verified c-Met as a target for brain cancer therapy.

In this work, human glioma cell line U87 was used for both *in vitro* and *in vivo* studies. This selection based on U87 cells have an autocrine Met signaling pathway and that neutralization of HGF is sufficient to induce tumor shrinkage *in vivo* [12] [13]. The bioluminescence imaging data showed the change of c-Met kinase activity with the treatment of HGF neutralizing antibody, which was correlated with the reduction of tumor growth as detected by MRI. This validated that bioluminescent Met reporter can be used as an indicator for c-Met targeted therapy. C-Met is involved in a variety of human malignants, including gastric cancer, colorectal carcinomas, melanomas, breast carcinomas[14]. For future study, this reporter assay can be adapted in different cancer models.

Activation of HGF/Met pathway has been seen in injured organs, such as liver, kidney or heart[15]. It indicates the defensive function of HGF/Met pathway. Bioluminescent Met reporter developed in this work has the ability to detect changes in Met status in response to the activation of HGF. So this reporter can be used to study the role of HGF/Met against tissue injury.

As cancer progression is usually linked to a combination of genetic alteration, it is impossible to develop therapies suitable for 'all' cancers. However, it has been found that inactivation of individual oncogene can lead to the reduction of tumor growth. Therefore individualized molecular diagnosis is needed to understand the specific gene alteration that could be targeted by therapy in current clinical diagnosis. Using this reporter assay as surrogate, one could validate c-Met as a target in cancer therapy and evaluate c-Met

status in response to treatment in preclinical trials. Compared to time-consuming dissection and histology, this reporter assay decreases the workload involved in tissue analysis and thereby speeds up the evaluation. It will greatly aid in the classification of the patient subset that would benefit from c-Met targeted therapy.

Scientists are aware that tumors are not homogeneous collection of cells. Cancer stem cells which initiate neoplasm have been identified and characterized. Targeting cancer stem cell population which is capable of generating tumors would bring eventual success to cancer therapies[16]. Therefore it will lead to major advances to understand molecular and biochemical pathways which are crucial for cancer stem cells. It has been shown that Met is linked to self-renewal signaling pathways[17,18]. Therefore, Met may be a target for cancer stem cell therapy. The traditional methodologies to detect phosphorylation of proteins include western blot using a phospho-specific antibody and *in vitro* kinase assays. However, cancer stem cells only occupy 1-2% of total cell population. These traditional methods are invasive, time consuming and need massive proteins to perform the analysis. In contrast, the reporter assay developed in this work can be used to monitor protein kinase activity repetitively in a small amount of cells at different times. In summary, bioluminescence reporter assays will facilitate the characterization of molecular targets in cancer stem cells, enable the screening of compounds which inhibit c-Met activation in cancer stem cells and pave the way for discovery of novel clinical therapies.

References

1. Hennessy, B.T., Smith, D.L., Ram, P.T., Lu, Y. & Mills, G.B. Exploiting the PI3K/AKT pathway for cancer drug discovery. *Nat Rev Drug Discov* **4**, 988-1004 (2005).

2. Manning, B.D. & Cantley, L.C. AKT/PKB signaling: navigating downstream. *Cell* **129**, 1261-74 (2007).

3. Garcia-Echeverria, C. & Sellers, W.R. Drug discovery approaches targeting the PI3K/Akt pathway in cancer. *Oncogene* **27**, 5511-26 (2008).

4. Yap, T.A. et al. Targeting the PI3K-AKT-mTOR pathway: progress, pitfalls, and promises. *Curr Opin Pharmacol* **8**, 393-412 (2008).

5. Chen, C.S. et al. NF-kappaB-activated tissue transglutaminase is involved in ethanol-induced hepatic injury and the possible role of propolis in preventing fibrogenesis. *Toxicology* **246**, 148-57 (2008).

6. Jiao, S. et al. Benzo(a)pyrene-caused increased G1-S transition requires the activation of c-Jun through p53-dependent PI-3K/Akt/ERK pathway in human embryo lung fibroblasts. *Toxicol Lett* **178**, 167-75 (2008).

7. Li, C. et al. Involvement of cyclin D1/CDK4 and pRb mediated by PI3K/AKT pathway activation in Pb2+ -induced neuronal death in cultured hippocampal neurons. *Toxicol Appl Pharmacol* **229**, 351-61 (2008).

8. Liu, Z., Yu, X. & Shaikh, Z.A. Rapid activation of ERK1/2 and AKT in human breast cancer cells by cadmium. *Toxicol Appl Pharmacol* **228**, 286-94 (2008).

9. Ouyang, W. et al. PI-3K/Akt pathway-dependent cyclin D1 expression is responsible for arsenite-induced human keratinocyte transformation. *Environ Health Perspect* **116**, 1-6 (2008).

10. Sandoval, M. et al. p53 response to arsenic exposure in epithelial cells: protein kinase B/Akt involvement. *Toxicol Sci* **99**, 126-40 (2007).

11. Zhang, L., Bhojani, M.S., Ross, B.D. & Rehemtulla, A. Enhancing Akt imaging through targeted reporter expression. *Mol Imaging* **7**, 168-74 (2008).

12. Burgess, T. et al. Fully human monoclonal antibodies to hepatocyte growth factor with therapeutic potential against hepatocyte growth factor/c-Met-dependent human tumors. *Cancer Res* **66**, 1721-9 (2006).

13. Kim, K.J. et al. Systemic anti-hepatocyte growth factor monoclonal antibody therapy induces the regression of intracranial glioma xenografts. *Clin Cancer Res* **12**, 1292-8 (2006).

14. Toschi, L. & Janne, P.A. Single-agent and combination therapeutic strategies to inhibit hepatocyte growth factor/MET signaling in cancer. *Clin Cancer Res* **14**, 5941-6 (2008).

15. Birchmeier, C., Birchmeier, W., Gherardi, E. & Vande Woude, G.F. Met, metastasis, motility and more. *Nat Rev Mol Cell Biol* **4**, 915-25 (2003).

16. Dean, M., Fojo, T. & Bates, S. Tumour stem cells and drug resistance. *Nat Rev Cancer* **5**, 275-84 (2005).

17. Boon, E.M., van der Neut, R., van de Wetering, M., Clevers, H. & Pals, S.T. Wnt signaling regulates expression of the receptor tyrosine kinase met in colorectal cancer. *Cancer Res* **62**, 5126-8 (2002).

18. Brembeck, F.H. et al. Essential role of BCL9-2 in the switch between beta-catenin's adhesive and transcriptional functions. *Genes Dev* **18**, 2225-30 (2004).